

# STIX imaging: overview of the methods and first results

Paolo Massa, MIDA, Department of Mathematics, University of Genoa

December 8 2021



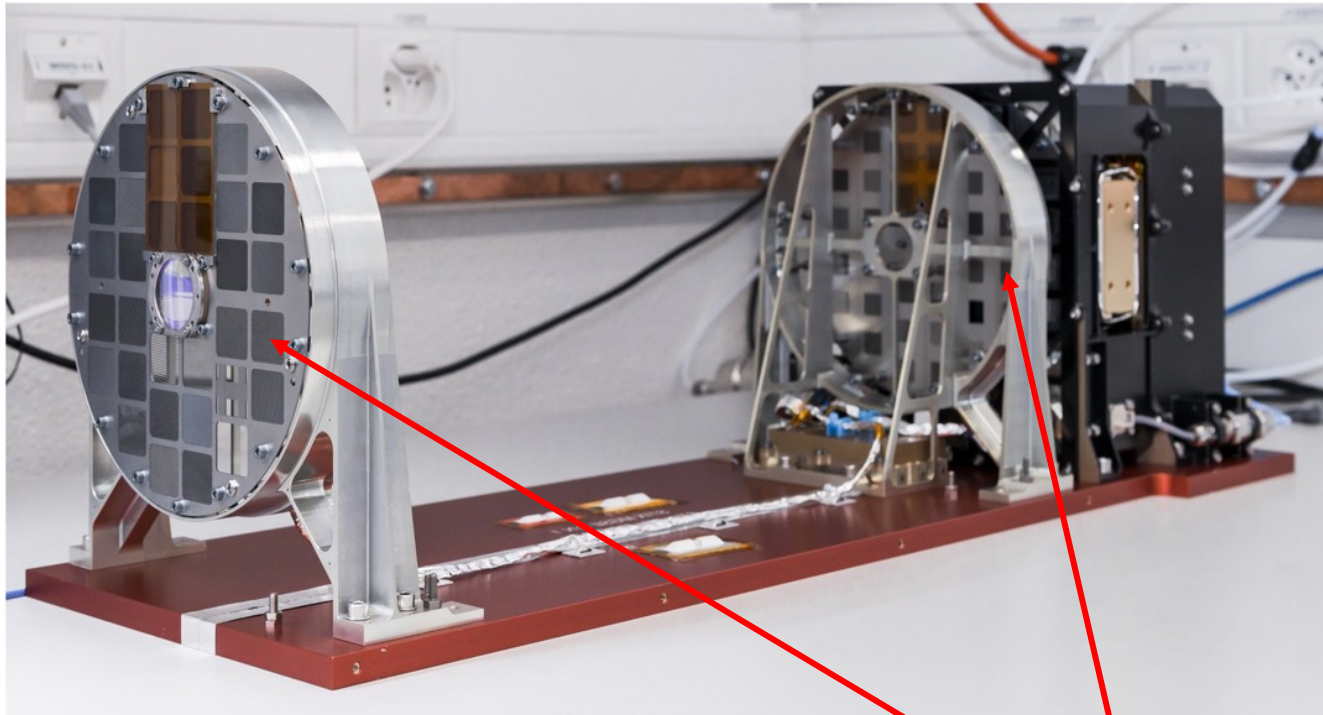
n|w



# Outline

- STIX imaging concept and visibility calibration
- Overview of the methods
- Results obtained on the X class flare (October 28 2021)

# The STIX imager



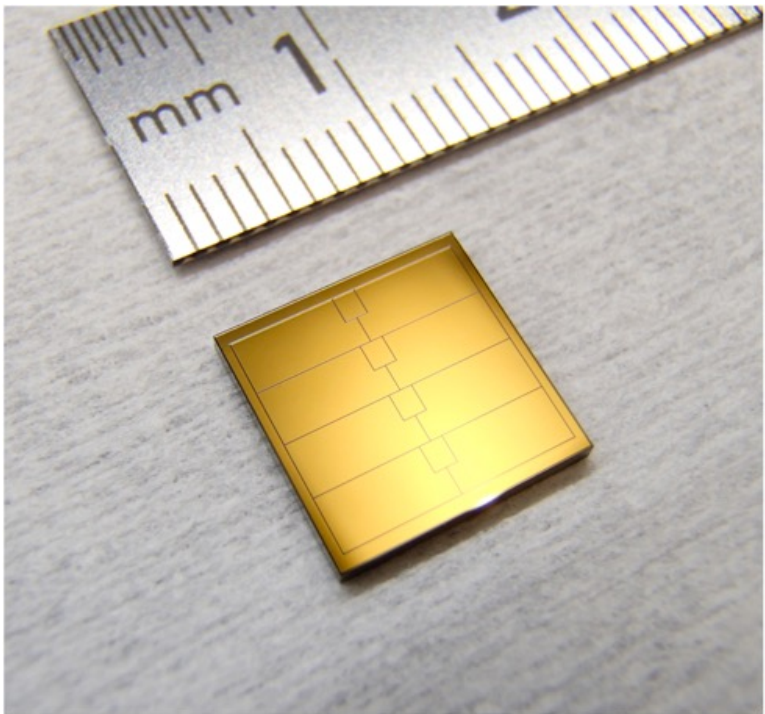
Krucker et al., 2020

subcollimator = front grid + rear grid + detector

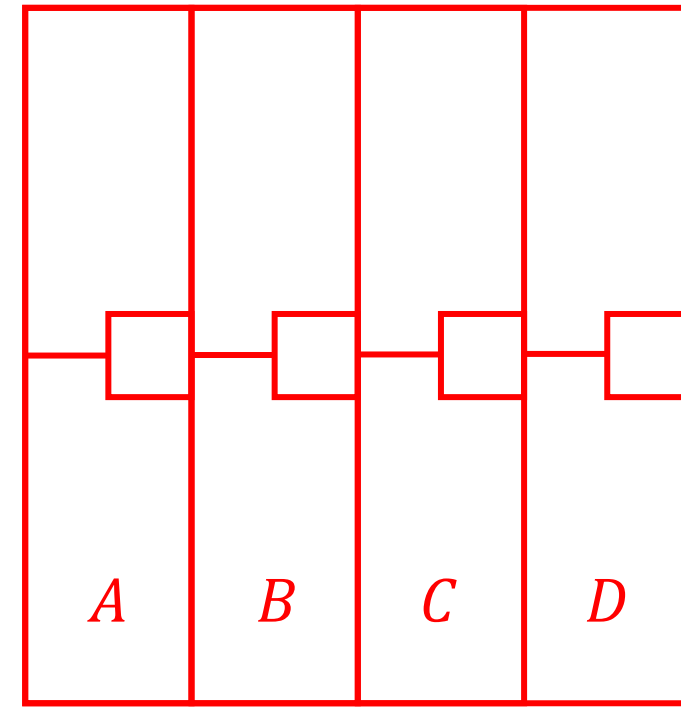
STIX consists of 32 subcollimators:

- 30 are used for imaging
- Coarse Flare Locator
- Background monitor

# The STIX imager



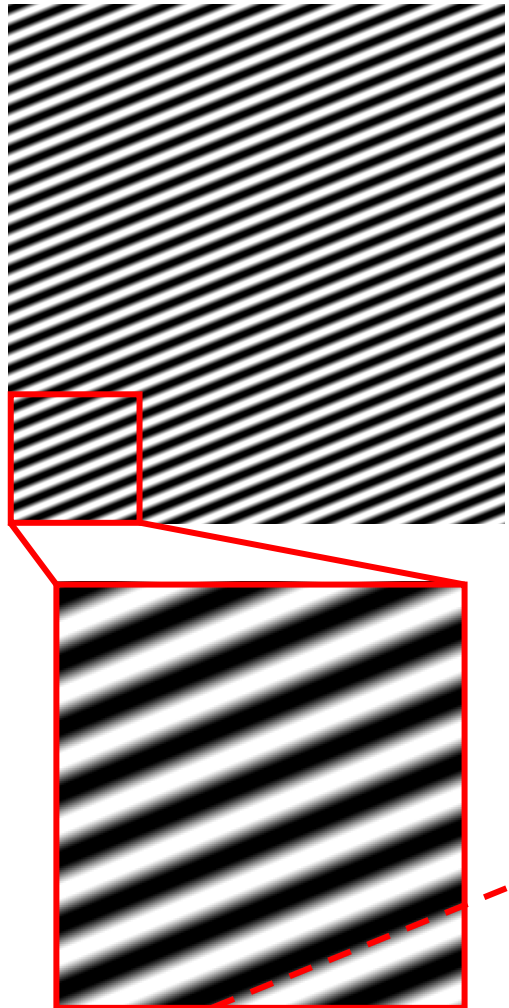
Krucker et al., 2020



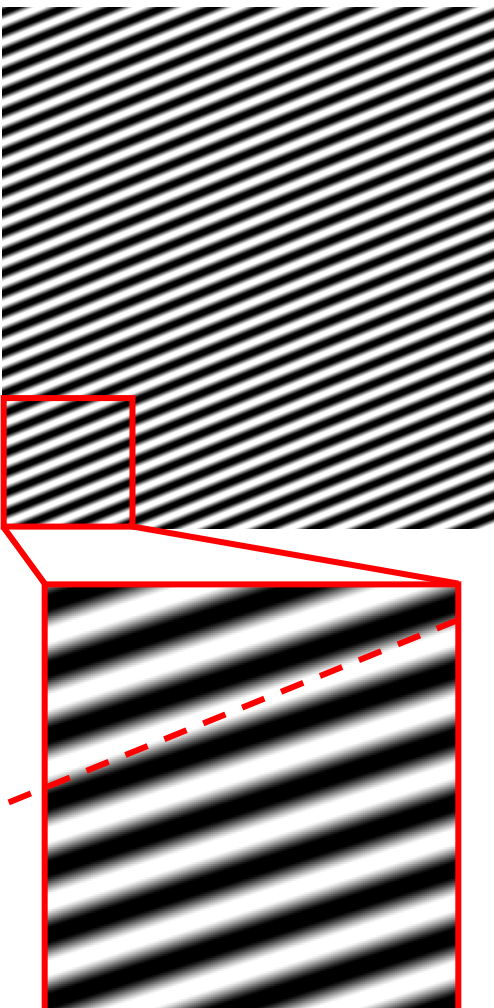
A, B, C and D: number of counts  
recorded by the detector pixels

# The STIX imaging concept

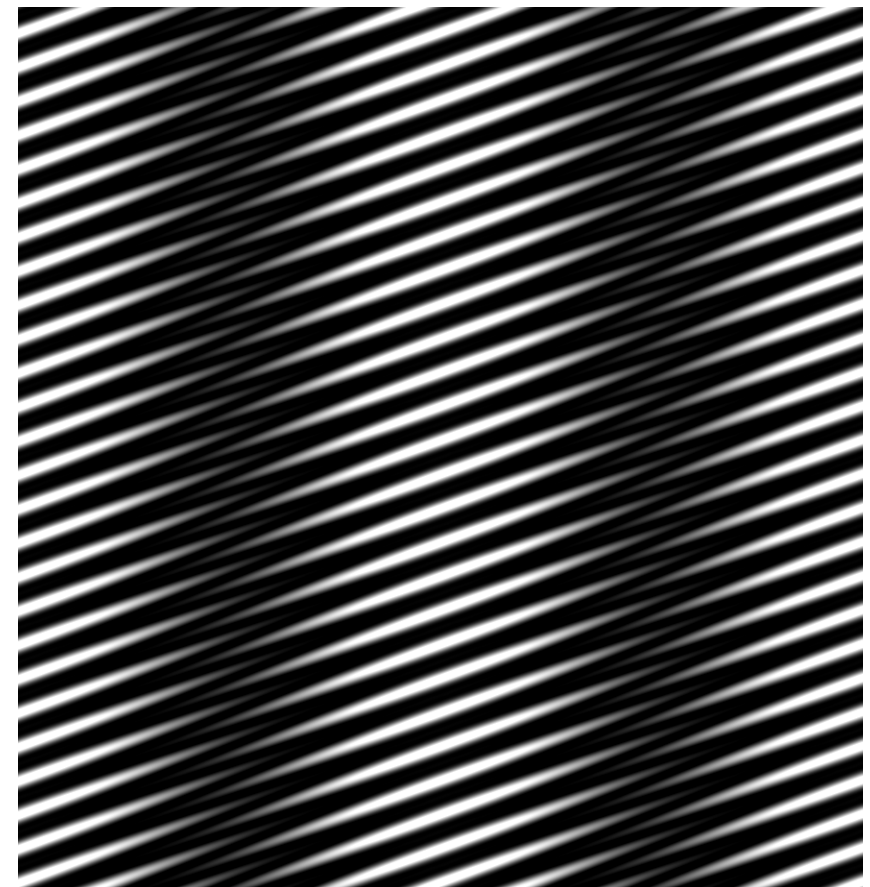
Front grid



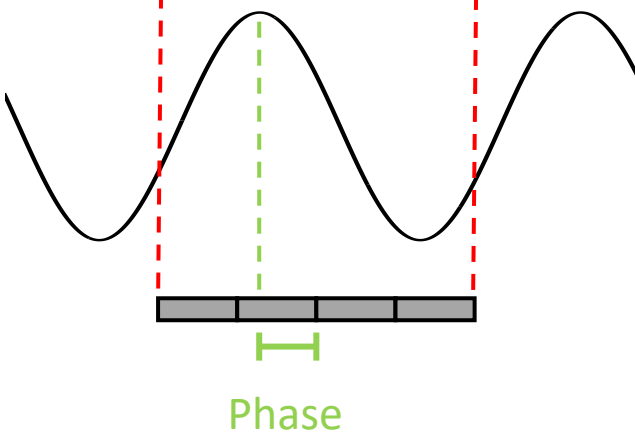
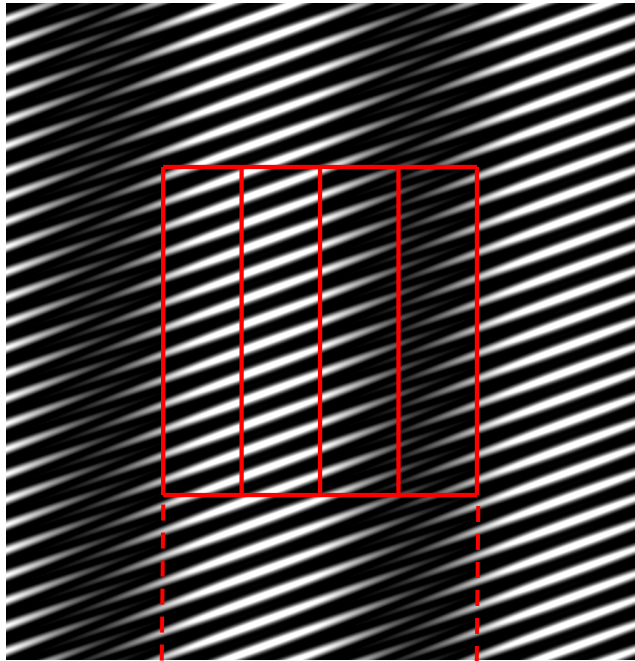
Rear grid



Moiré pattern



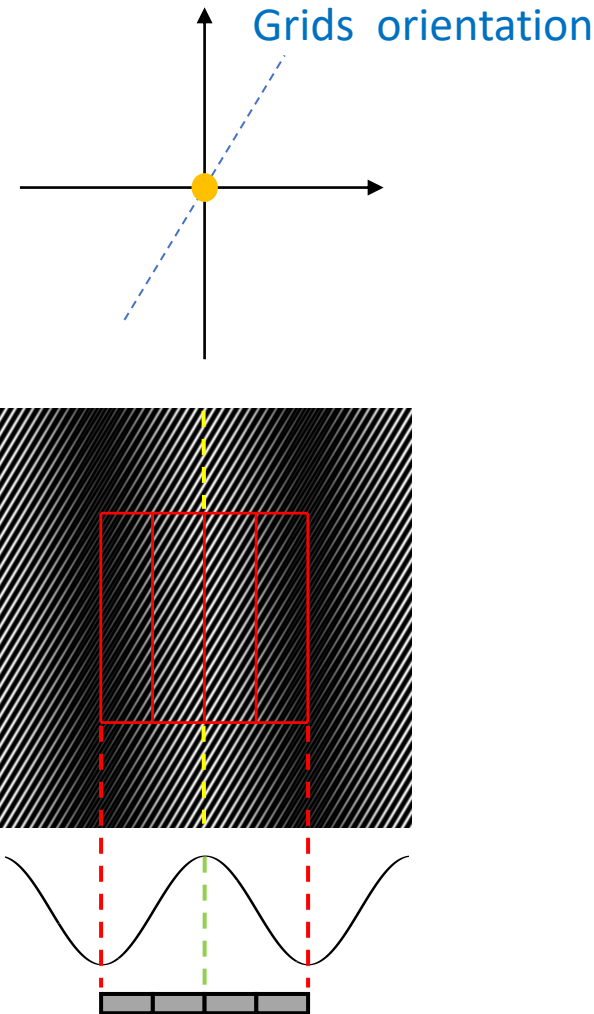
# The STIX imaging concept



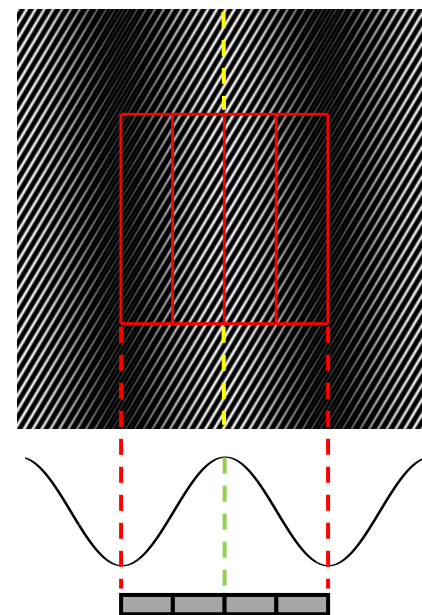
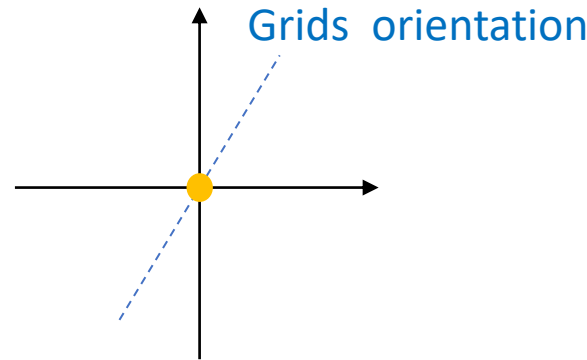
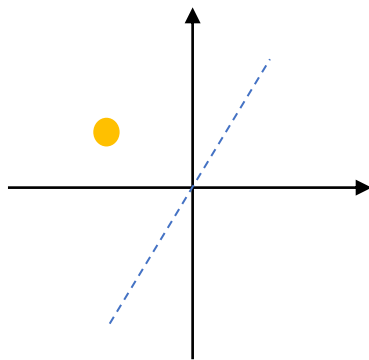
- Moiré pattern: sinusoidal wave with period equal to the detector width
- Amplitude and phase of the pattern → amplitude and phase of a Fourier component of the photon flux (**visibility**)



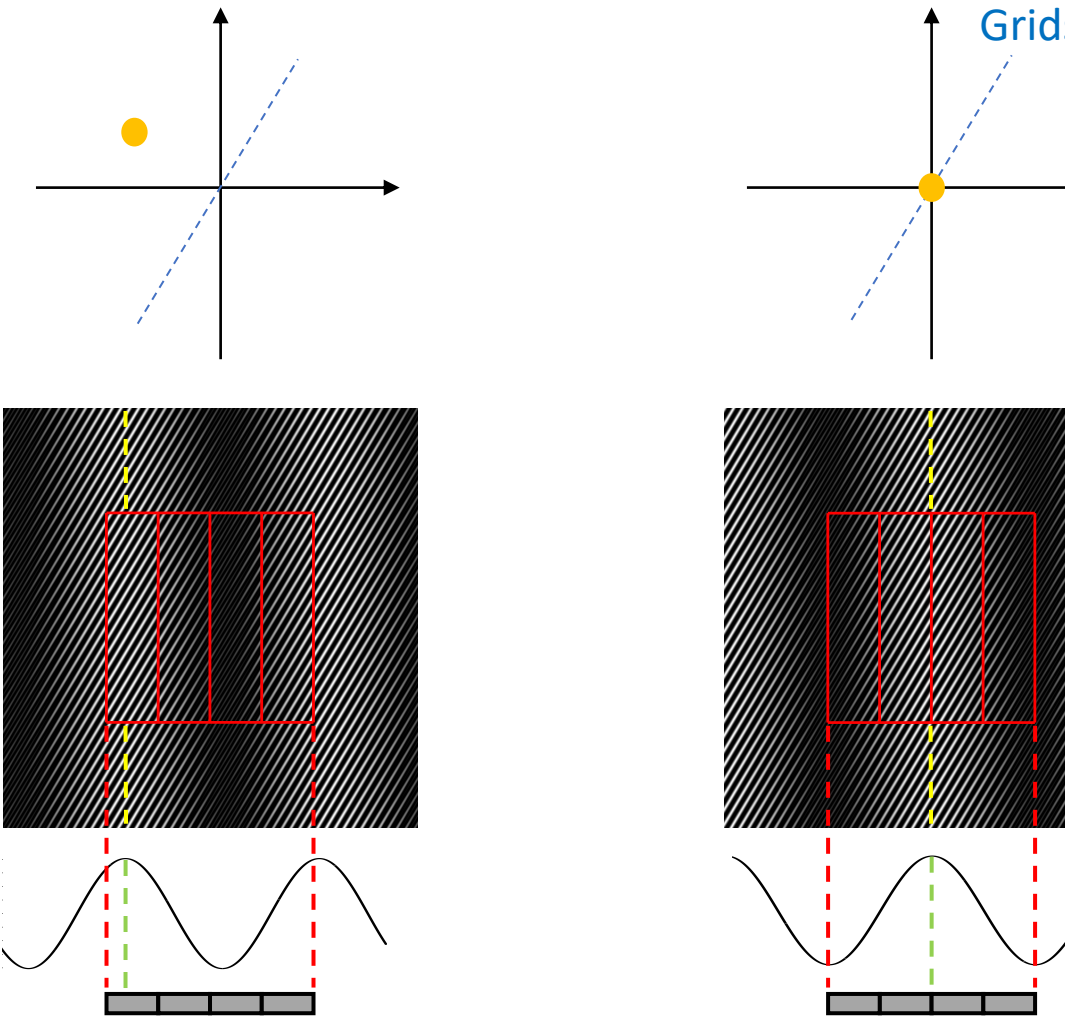
# The STIX imaging concept



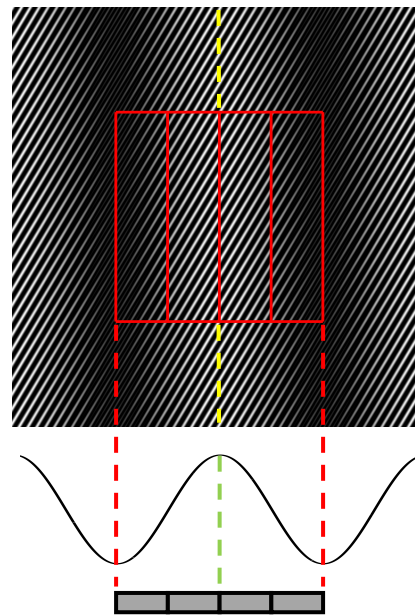
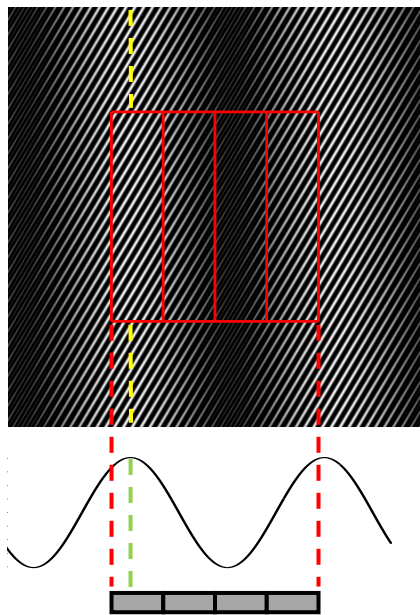
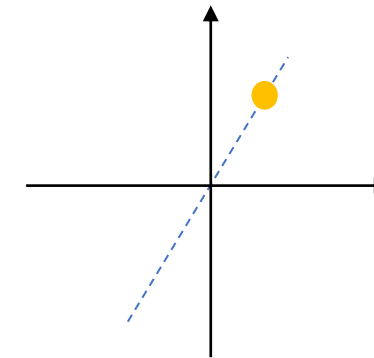
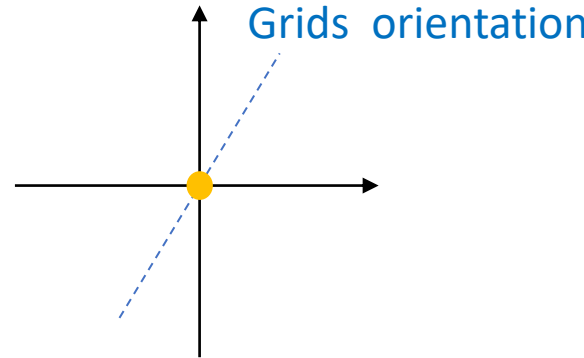
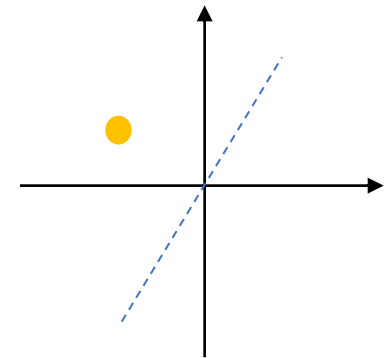
# The STIX imaging concept



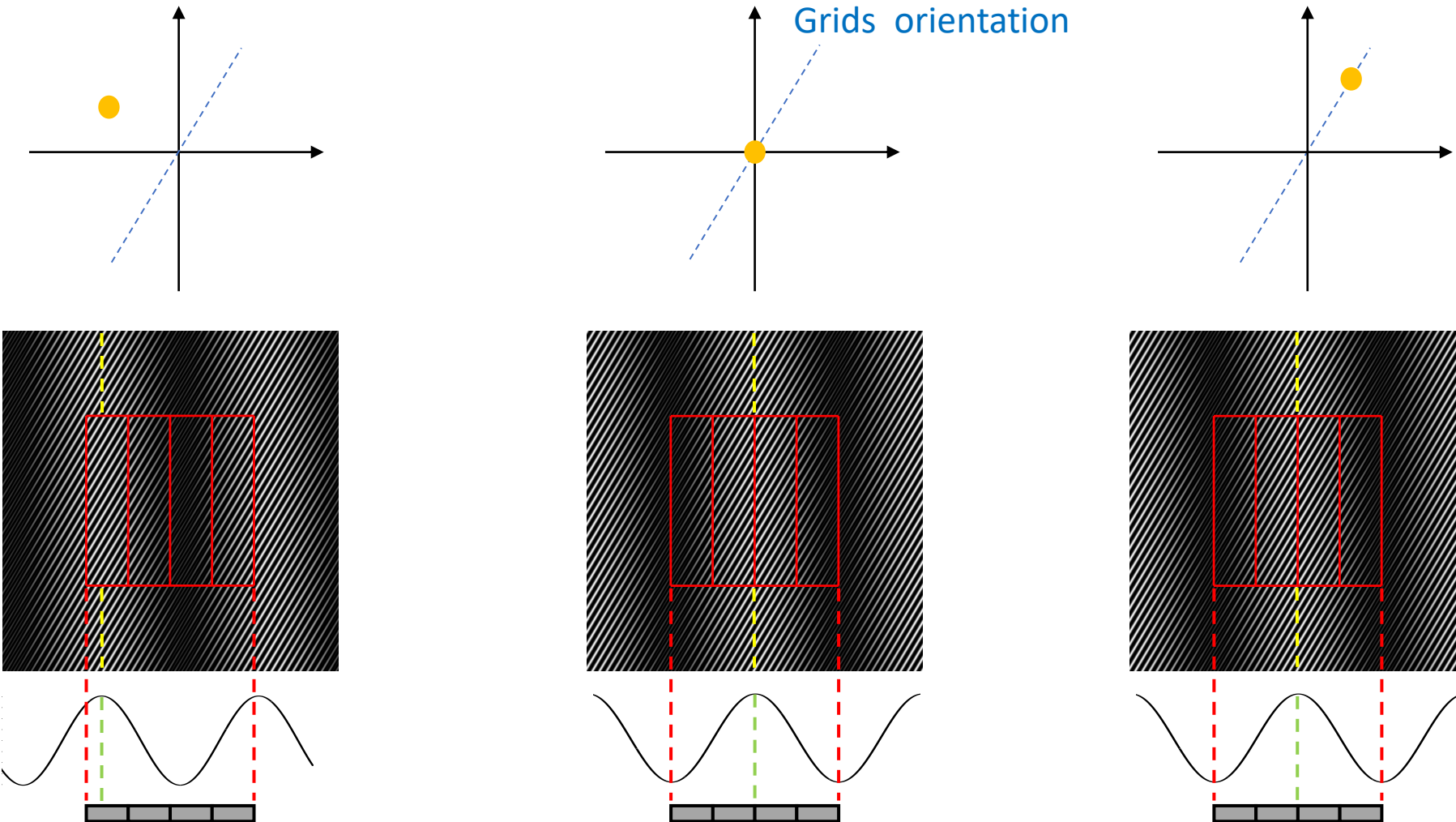
# The STIX imaging concept



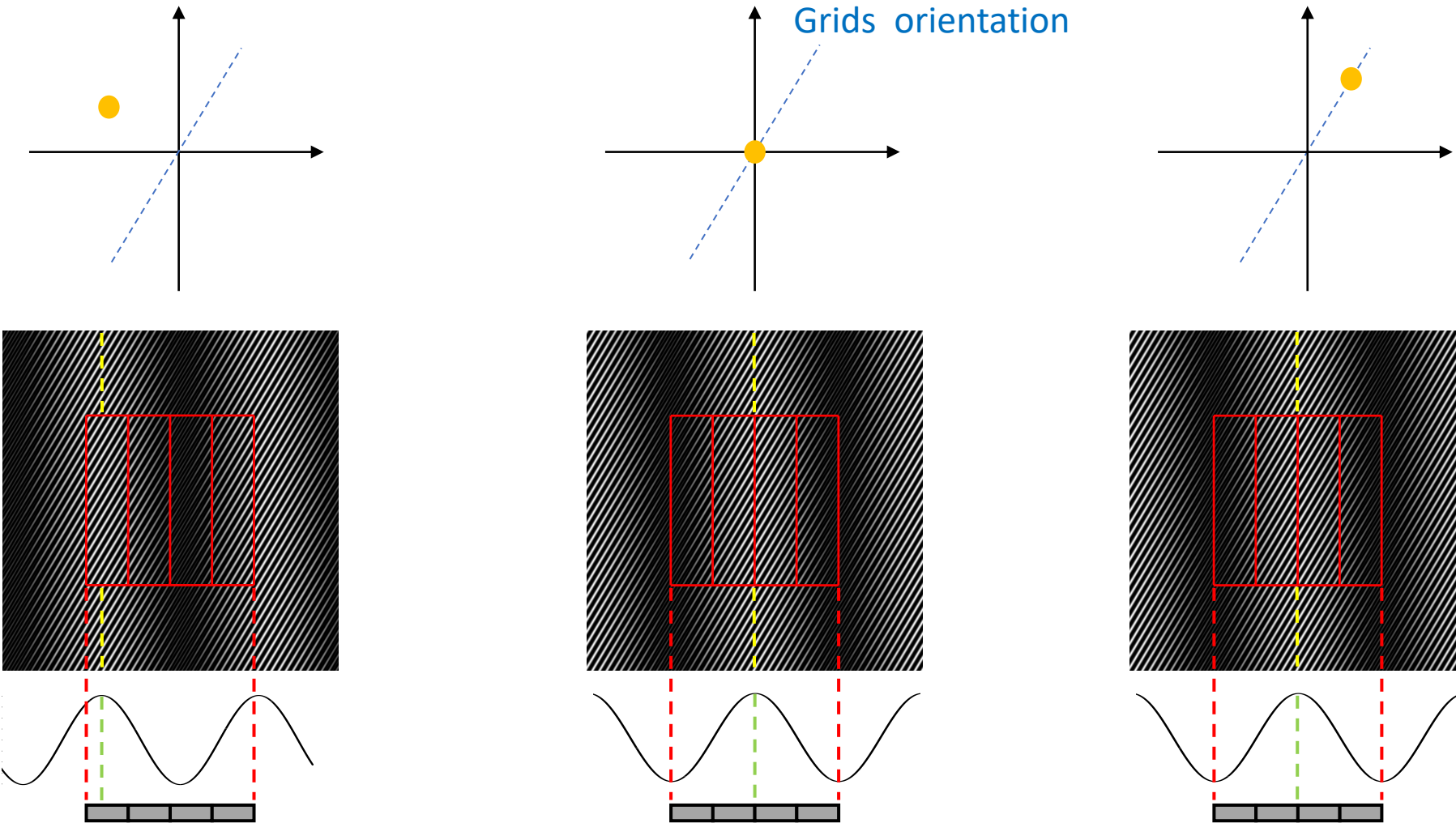
# The STIX imaging concept



# The STIX imaging concept

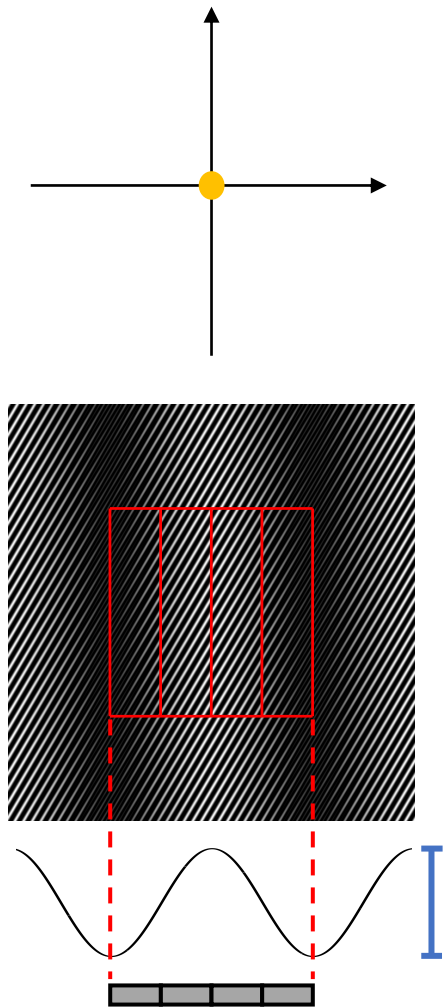


# The STIX imaging concept

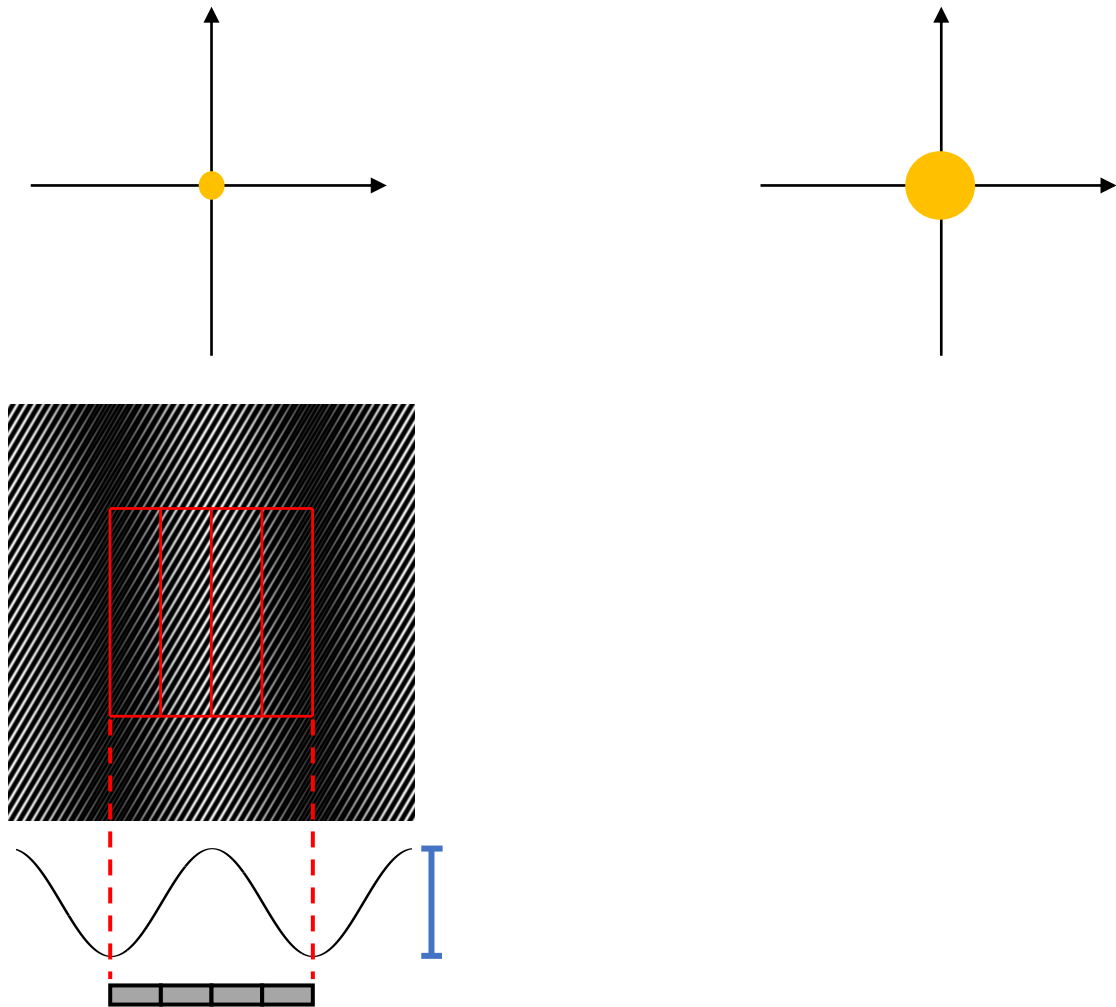


The phase of the Moiré pattern is sensitive to specific directions

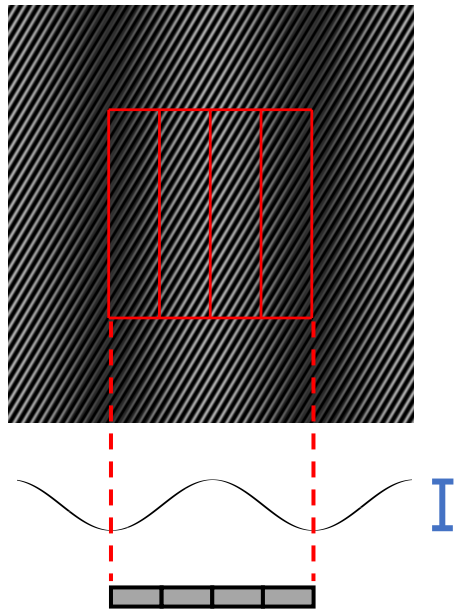
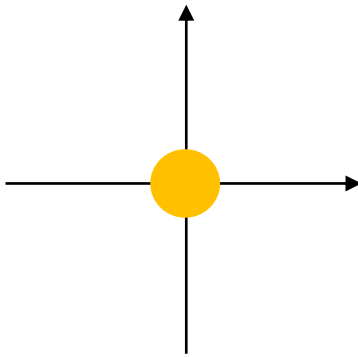
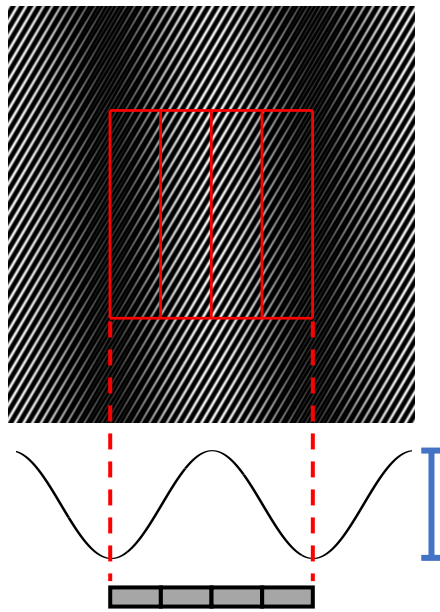
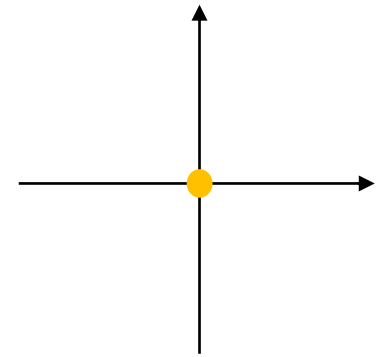
# The STIX imaging concept



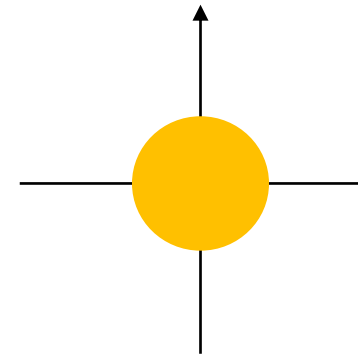
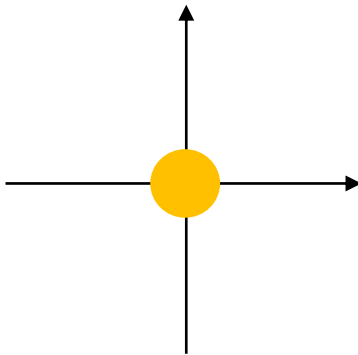
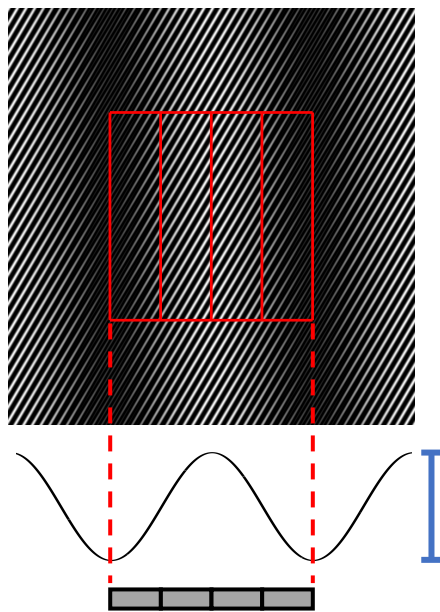
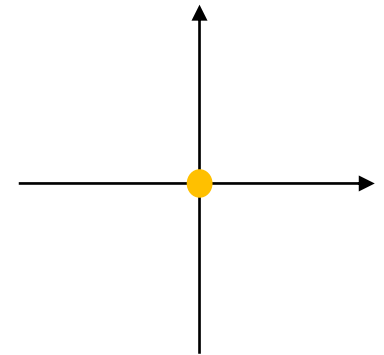
# The STIX imaging concept



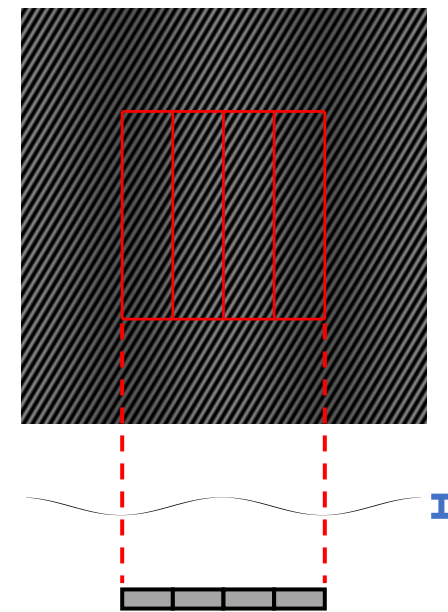
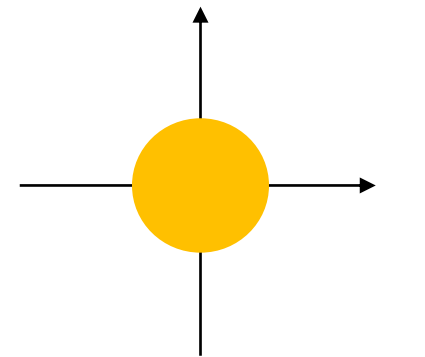
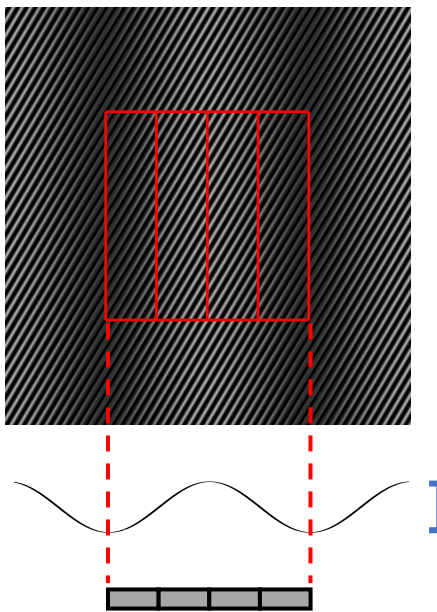
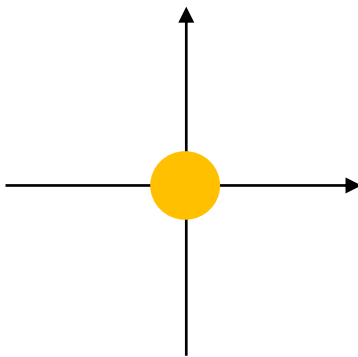
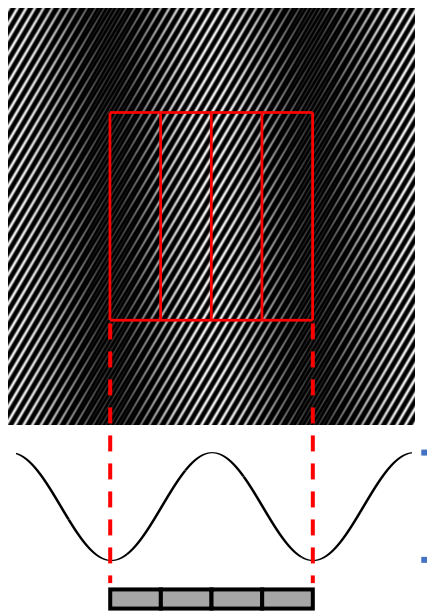
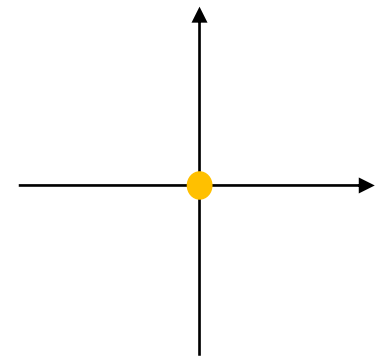
# The STIX imaging concept



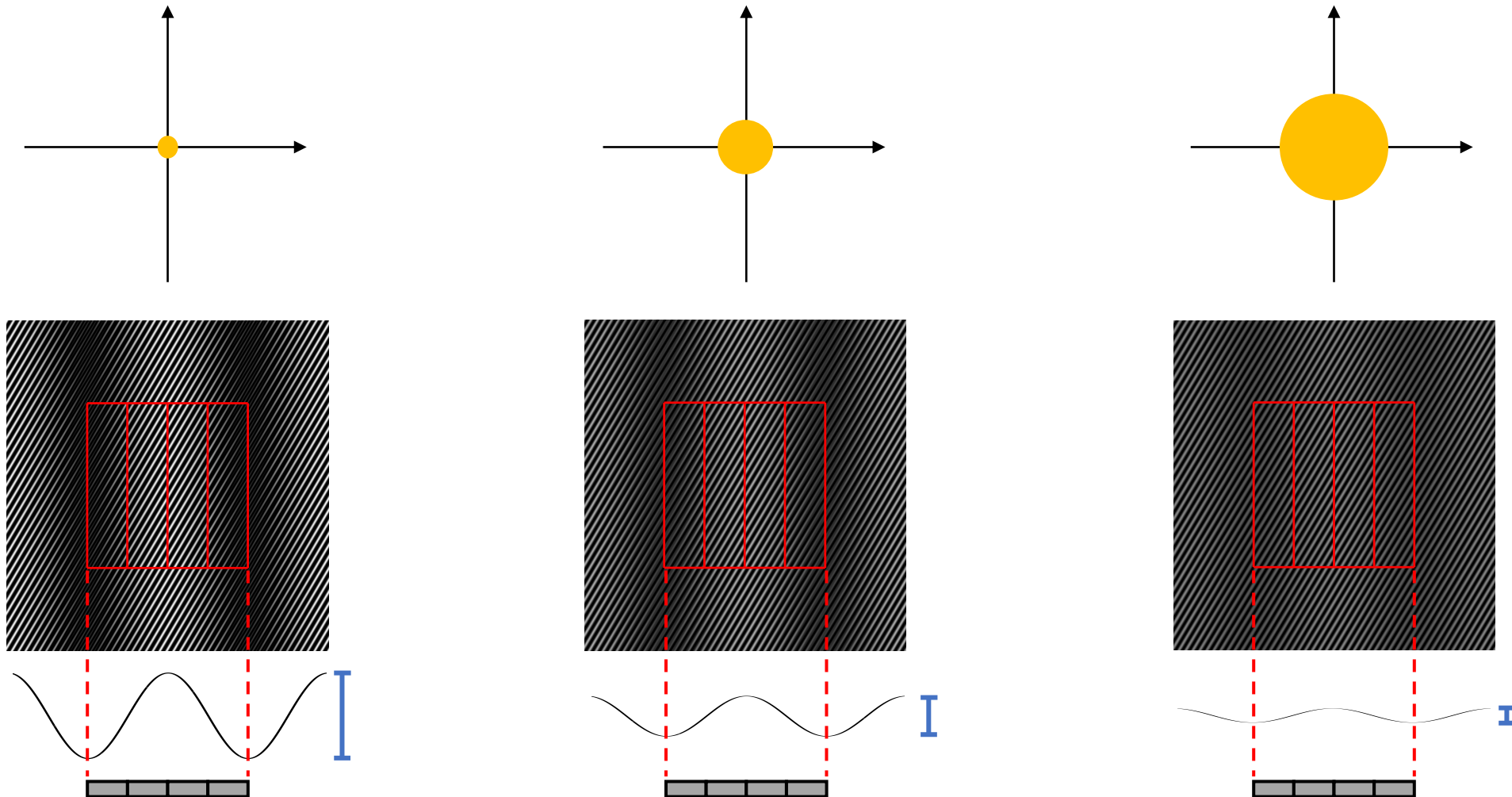
# The STIX imaging concept



# The STIX imaging concept



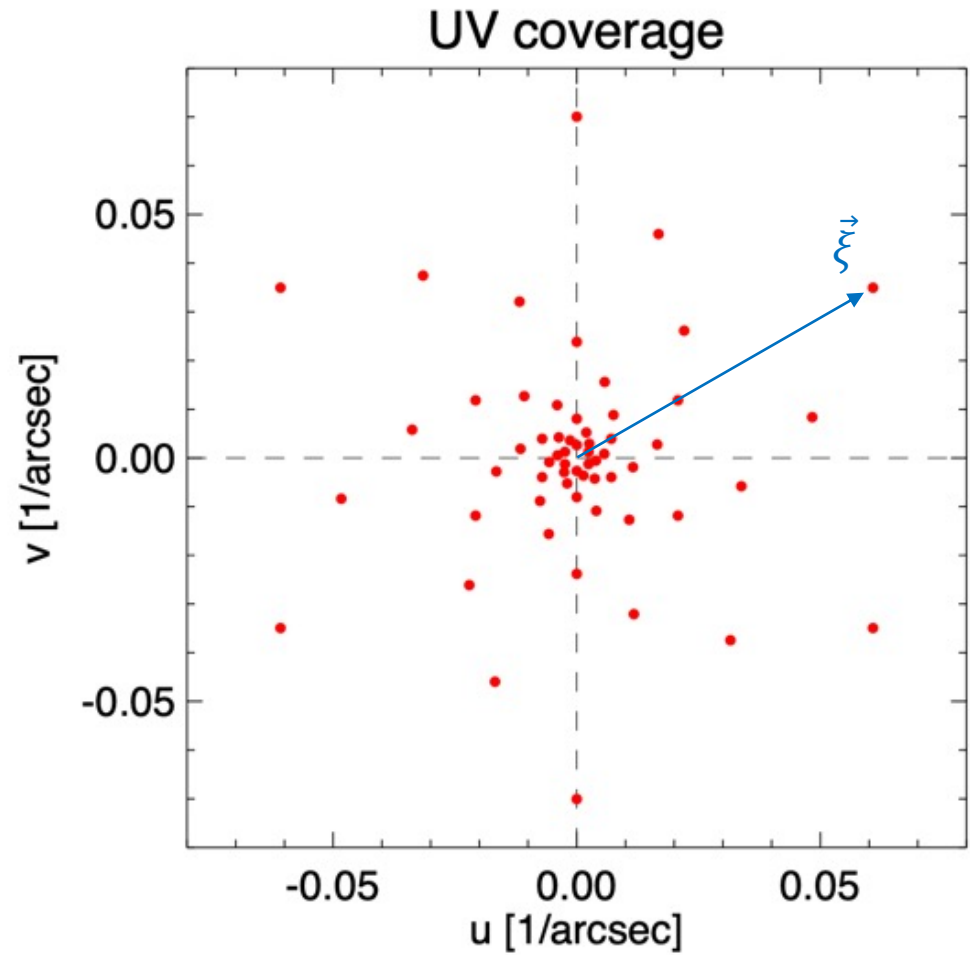
# The STIX imaging concept



The amplitude of the Moiré pattern is sensitive to the source size

# The STIX imaging concept

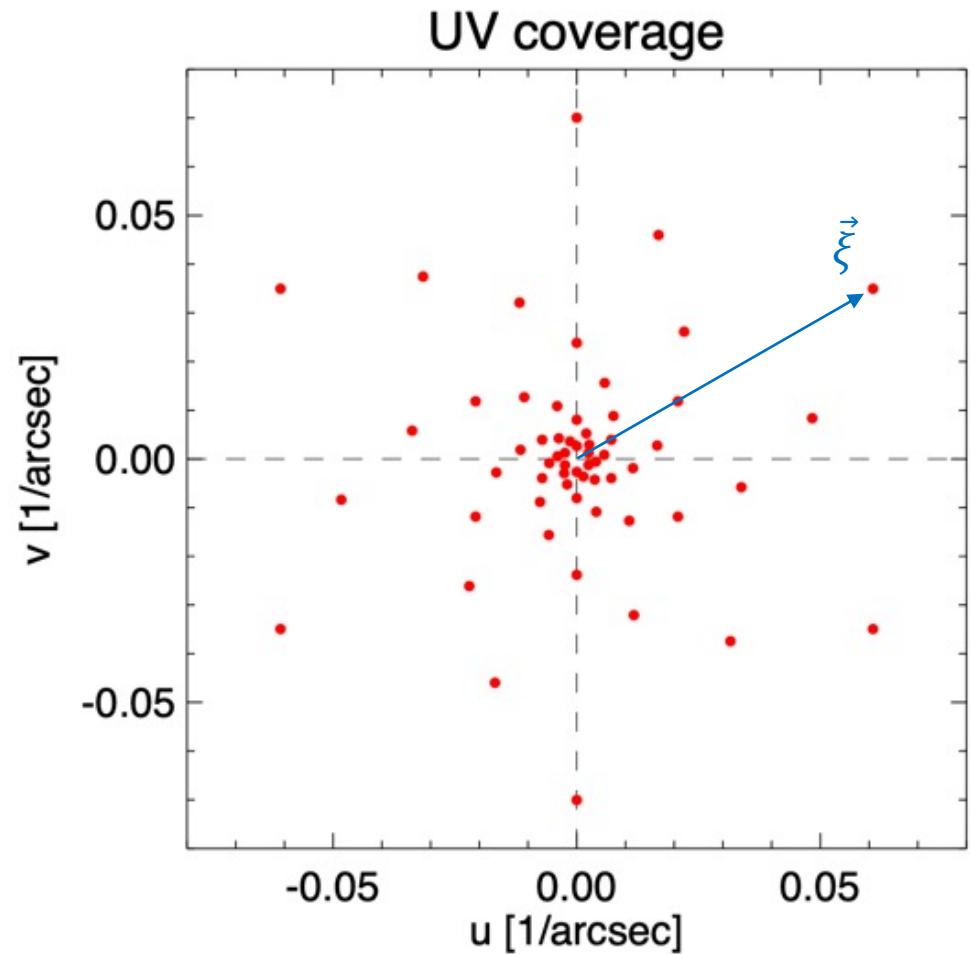
- Each subcollimator measures a complex visibility value  $V$  corresponding to an angular frequency  $\vec{\xi} = (u, v)$



Krucker et al., 2020

# The STIX imaging concept

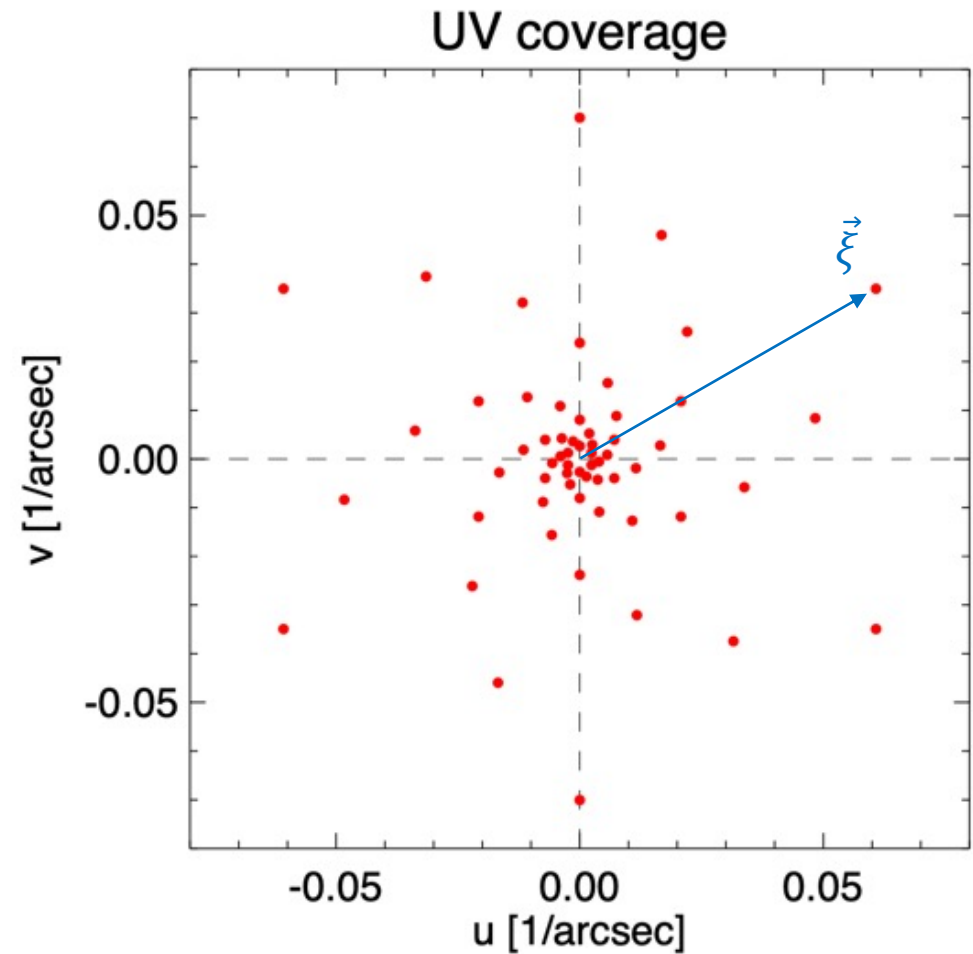
- Each subcollimator measures a complex visibility value  $V$  corresponding to an angular frequency  $\vec{\xi} = (u, v)$
- The direction of  $\vec{\xi}$  is perpendicular to the grid orientation



Krucker et al., 2020

# The STIX imaging concept

- Each subcollimator measures a complex visibility value  $V$  corresponding to an angular frequency  $\vec{\xi} = (u, v)$
- The direction of  $\vec{\xi}$  is perpendicular to the grid orientation
- The norm of  $\vec{\xi}$  is inversely proportional to pitch width



Krucker et al., 2020

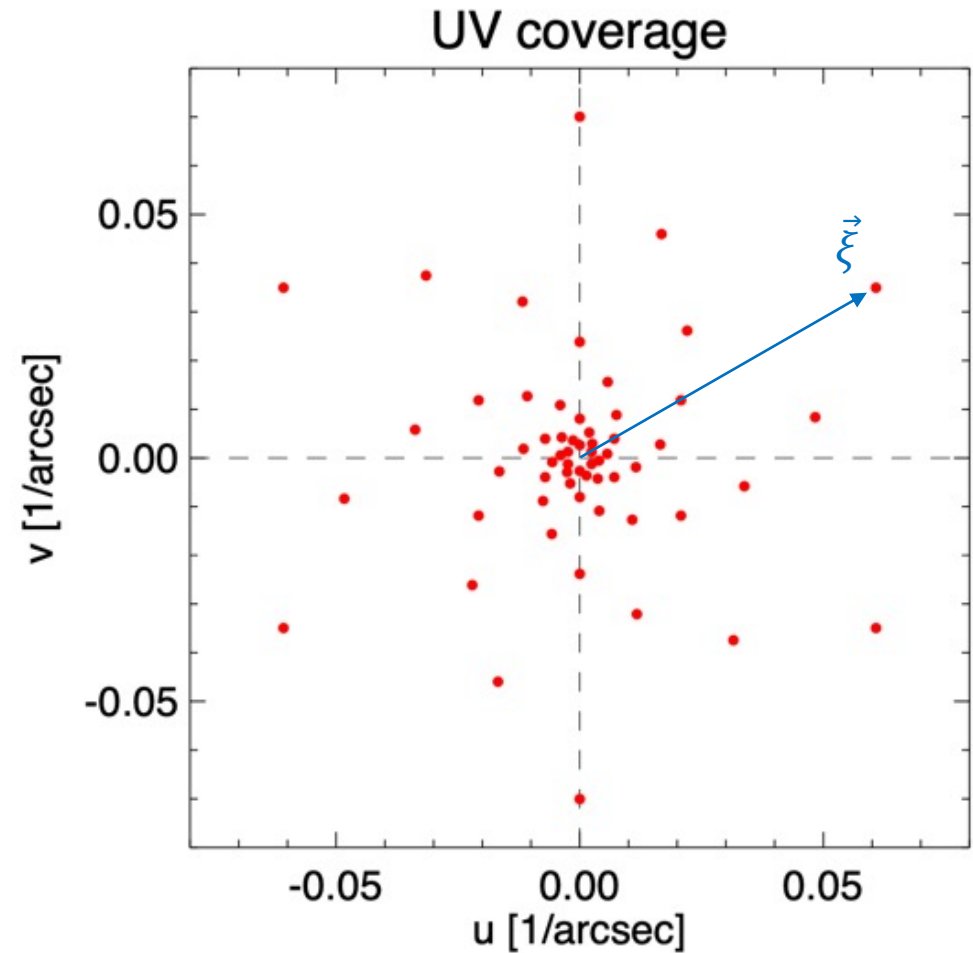
# The STIX imaging concept

- Each subcollimator measures a complex visibility value  $V$  corresponding to an angular frequency  $\vec{\xi} = (u, v)$
- The direction of  $\vec{\xi}$  is perpendicular to the grid orientation
- The norm of  $\vec{\xi}$  is inversely proportional to pitch width
- The visibility amplitude and phase are  $|V|$  and  $\phi$  such that

$$|V| \propto \sqrt{(C - A)^2 + (D - B)^2}$$

$$\phi = \text{atan}\left(\frac{D - B}{C - A}\right) + 45^\circ + \phi_{\text{calib}}$$

where  $\phi_{\text{calib}}$  is a phase calibration factor



Krucker et al., 2020

# Visibility calibration

## **Amplitude calibration:**

- background subtraction
- grid transmission (including the flare location)
- ELUT
- livetime

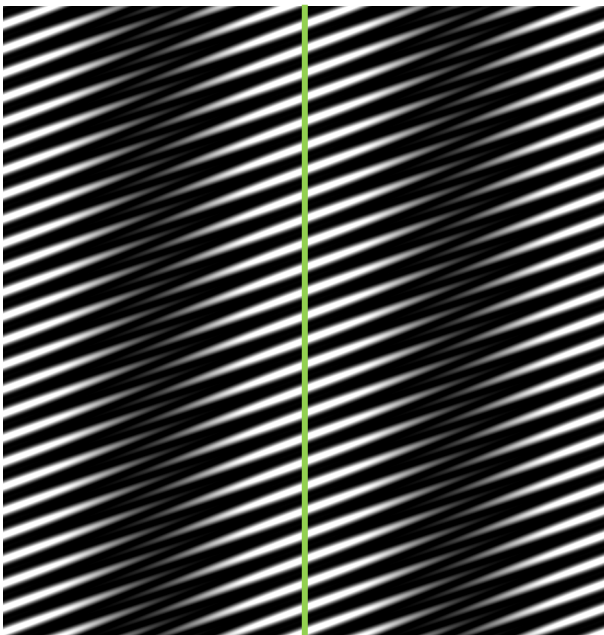
**Phase calibration:** keeps into account the grid geometry (see Matej's report) and possible distortions

# Visibility calibration

## Amplitude calibration:

- background subtraction
- grid transmission (including the flare location)
- ELUT
- livetime

**Phase calibration:** keeps into account the grid geometry (see Matej's report) and possible distortions

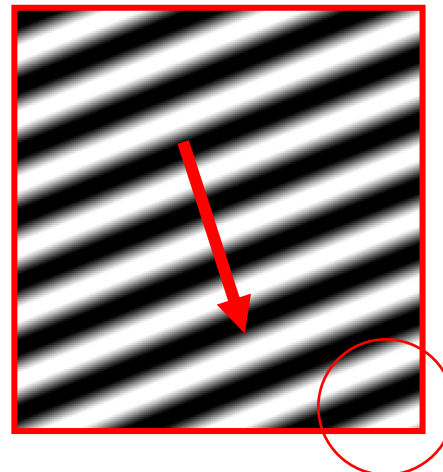
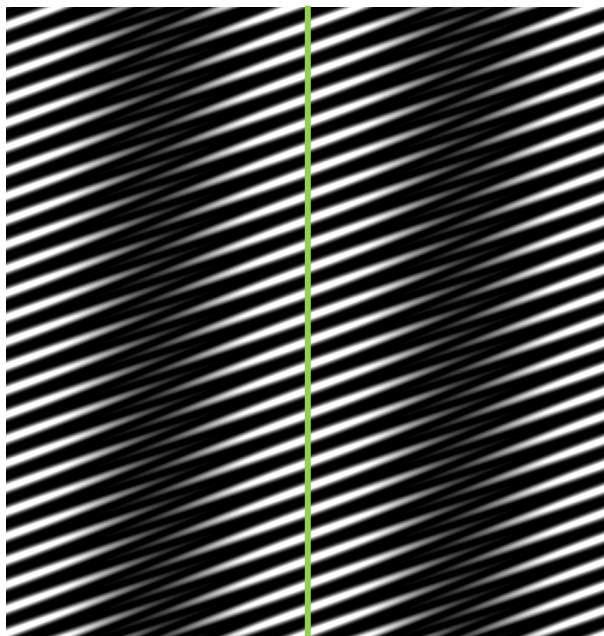


# Visibility calibration

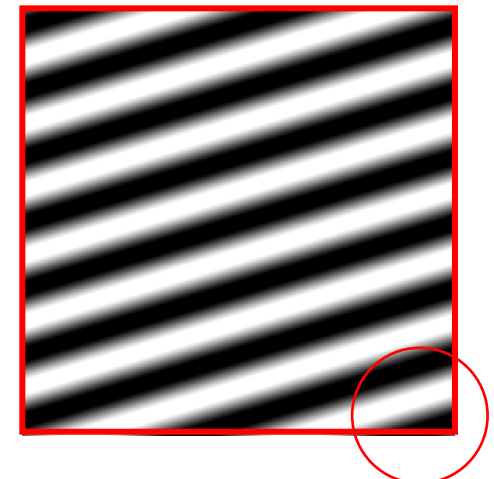
## Amplitude calibration:

- background subtraction
- grid transmission (including the flare location)
- ELUT
- livetime

**Phase calibration:** keeps into account the grid geometry (see Matej's report) and possible distortions



Shift front grid

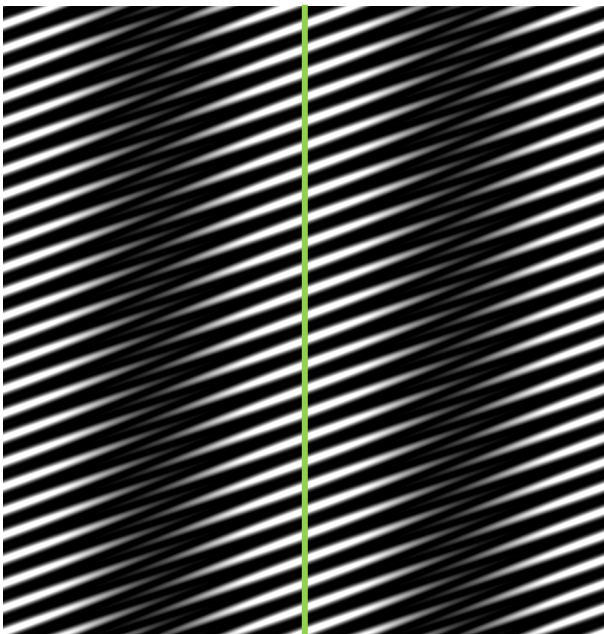


# Visibility calibration

## Amplitude calibration:

- background subtraction
- grid transmission (including the flare location)
- ELUT
- livetime

**Phase calibration:** keeps into account the grid geometry (see Matej's report) and possible distortions



Shift front grid  
→

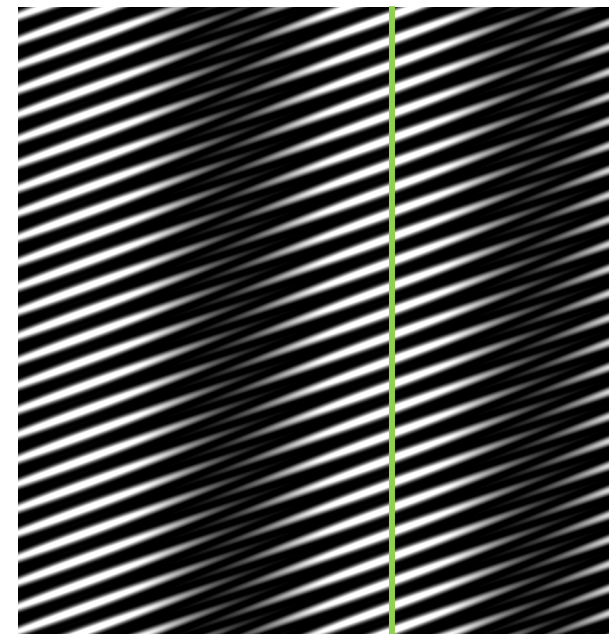


# Image reconstruction problem

Image reconstruction problem for STIX:

$$F\mathbf{x} = \mathbf{V}$$

Where:

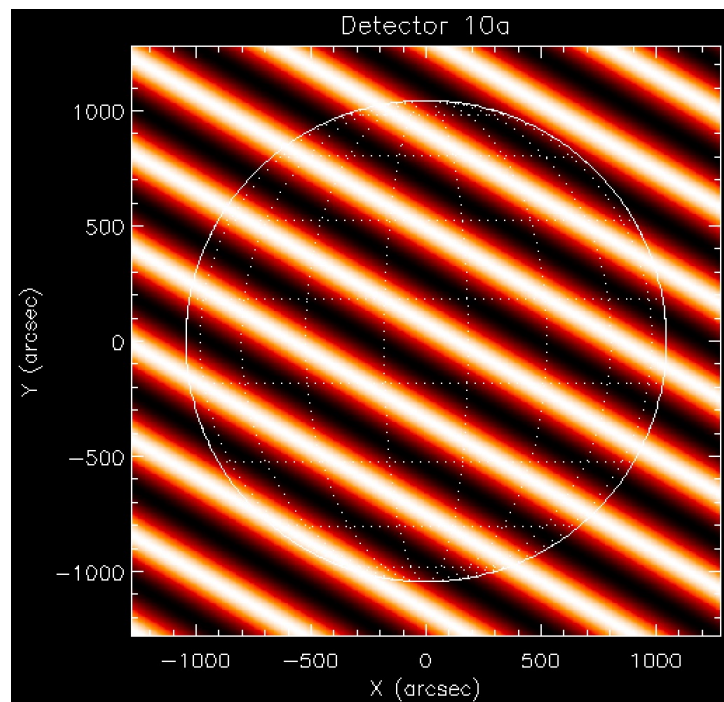
- $\mathbf{x}$  is the image to reconstruct
- $F$  is the Fourier transform
- $\mathbf{V}$  is the complex array of visibilities

This problem is analogous to the RHESSI one: we can use the same algorithms

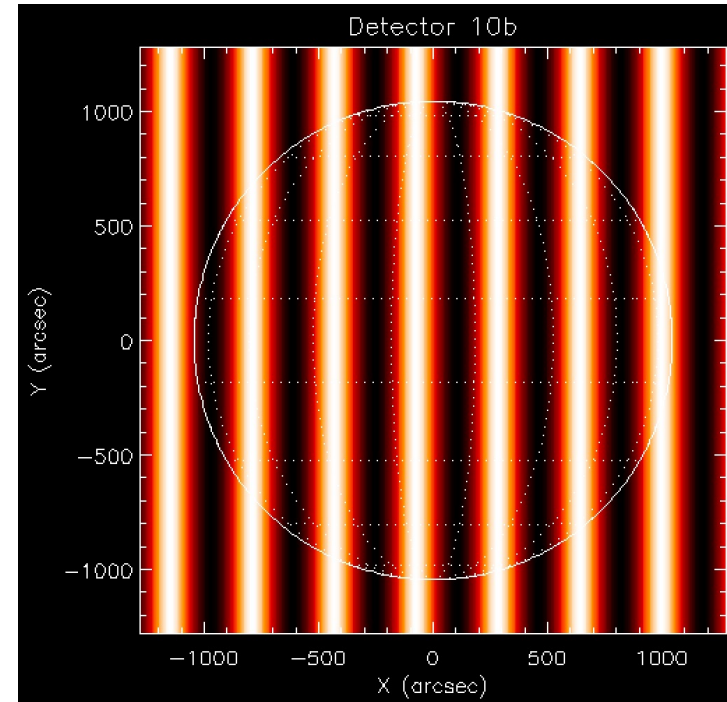
# Back projection (Mertz et al., 1986)

Visibility phase and amplitude → Phase and amplitude of a sinusoidal wave on the Sun

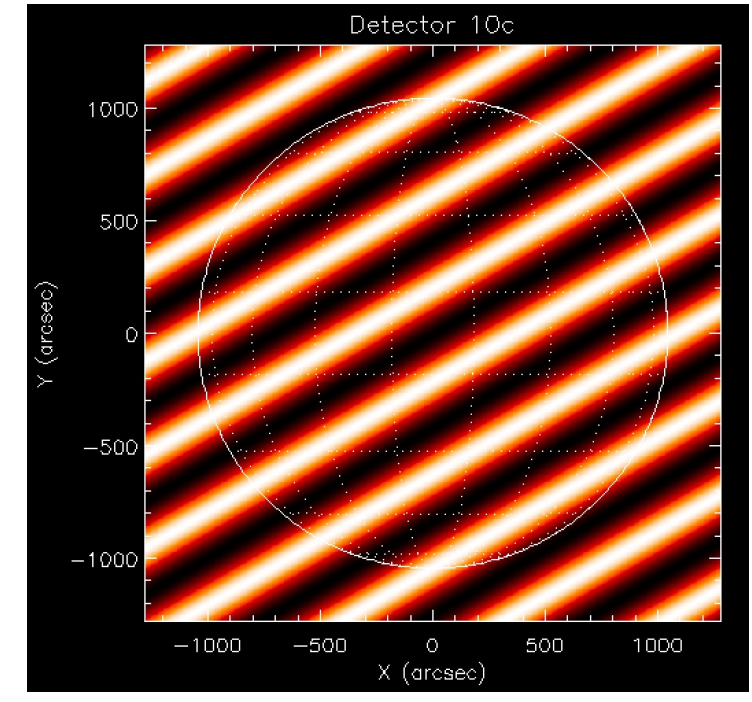
10a



10b



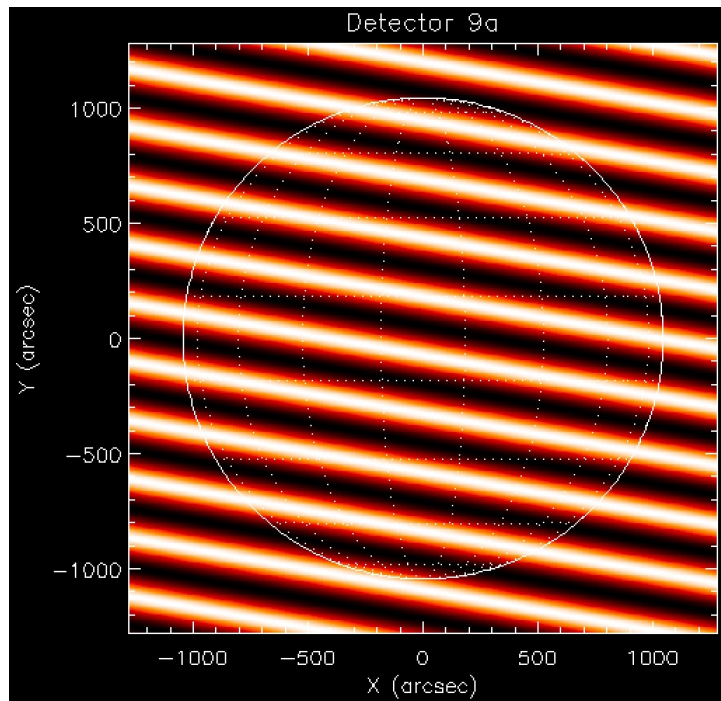
10c



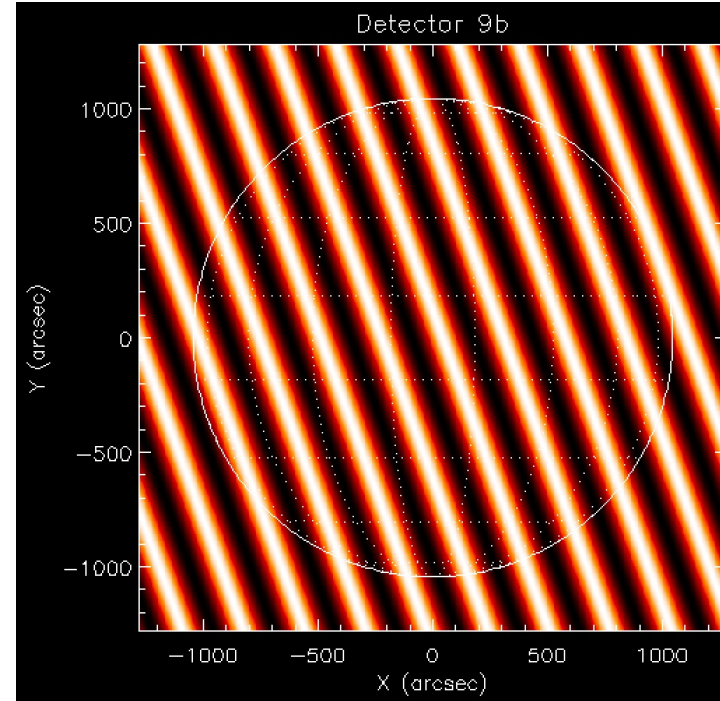
# Back projection (Mertz et al., 1986)

Visibility phase and amplitude → Phase and amplitude of a sinusoidal wave on the Sun

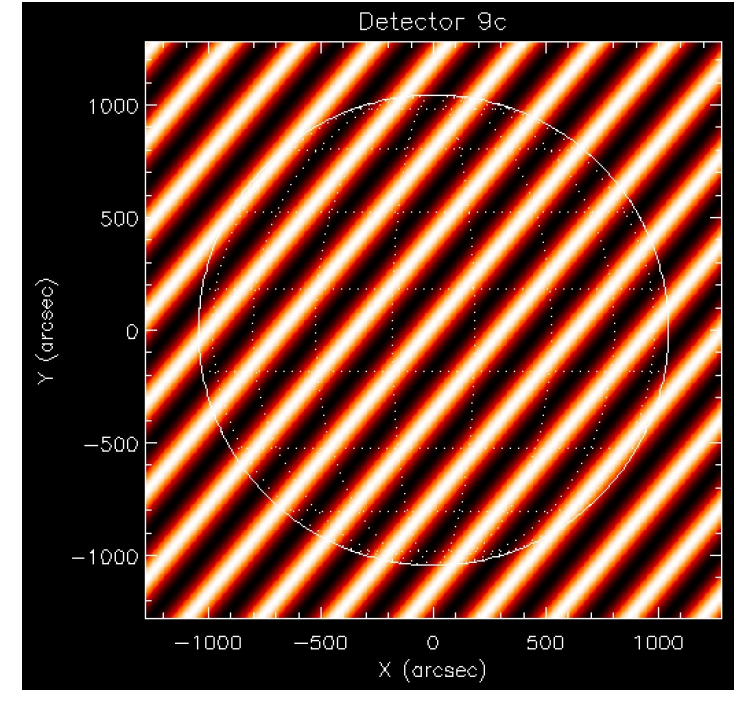
9a



9b



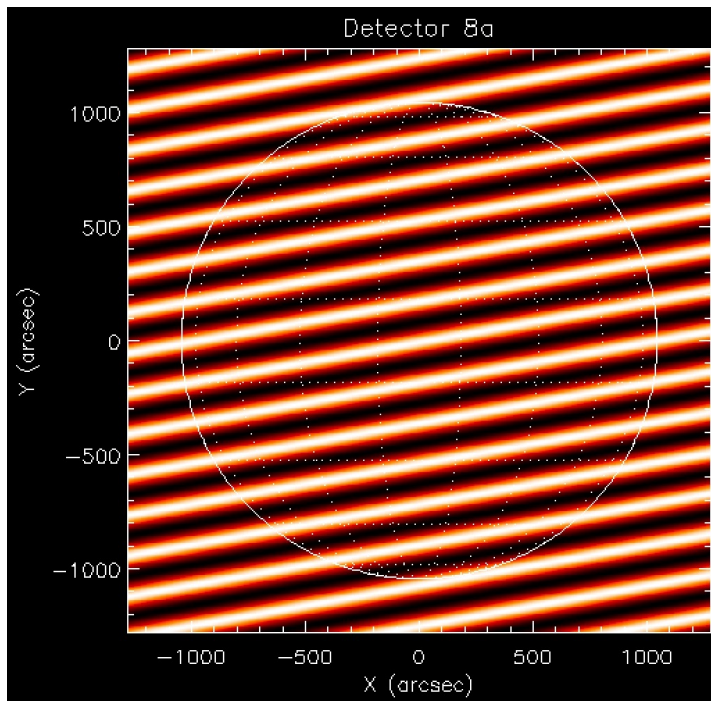
9c



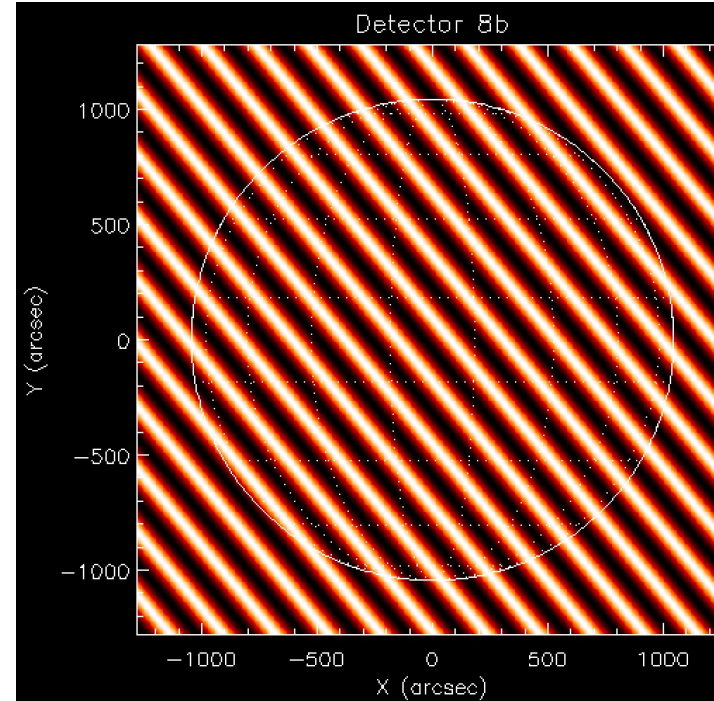
# Back projection (Mertz et al., 1986)

Visibility phase and amplitude → Phase and amplitude of a sinusoidal wave on the Sun

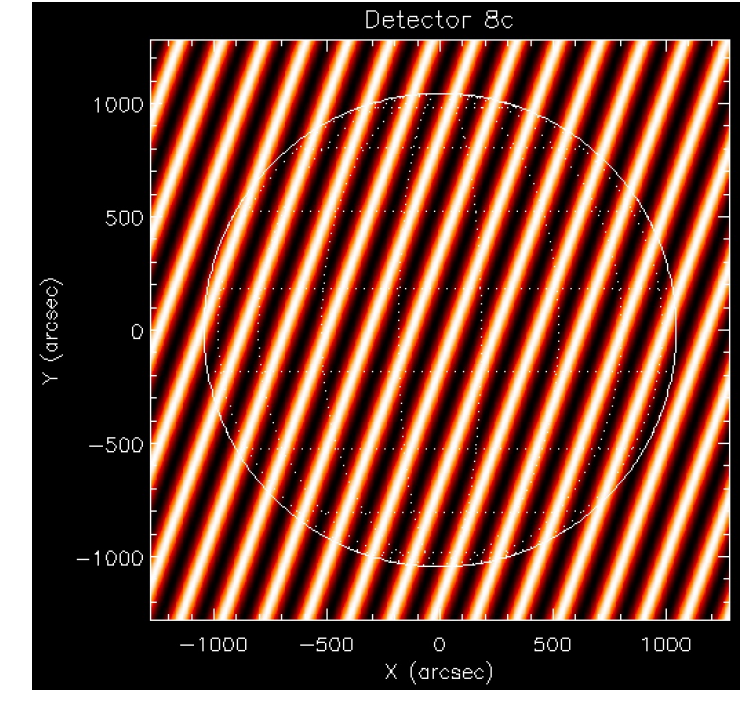
8a



8b

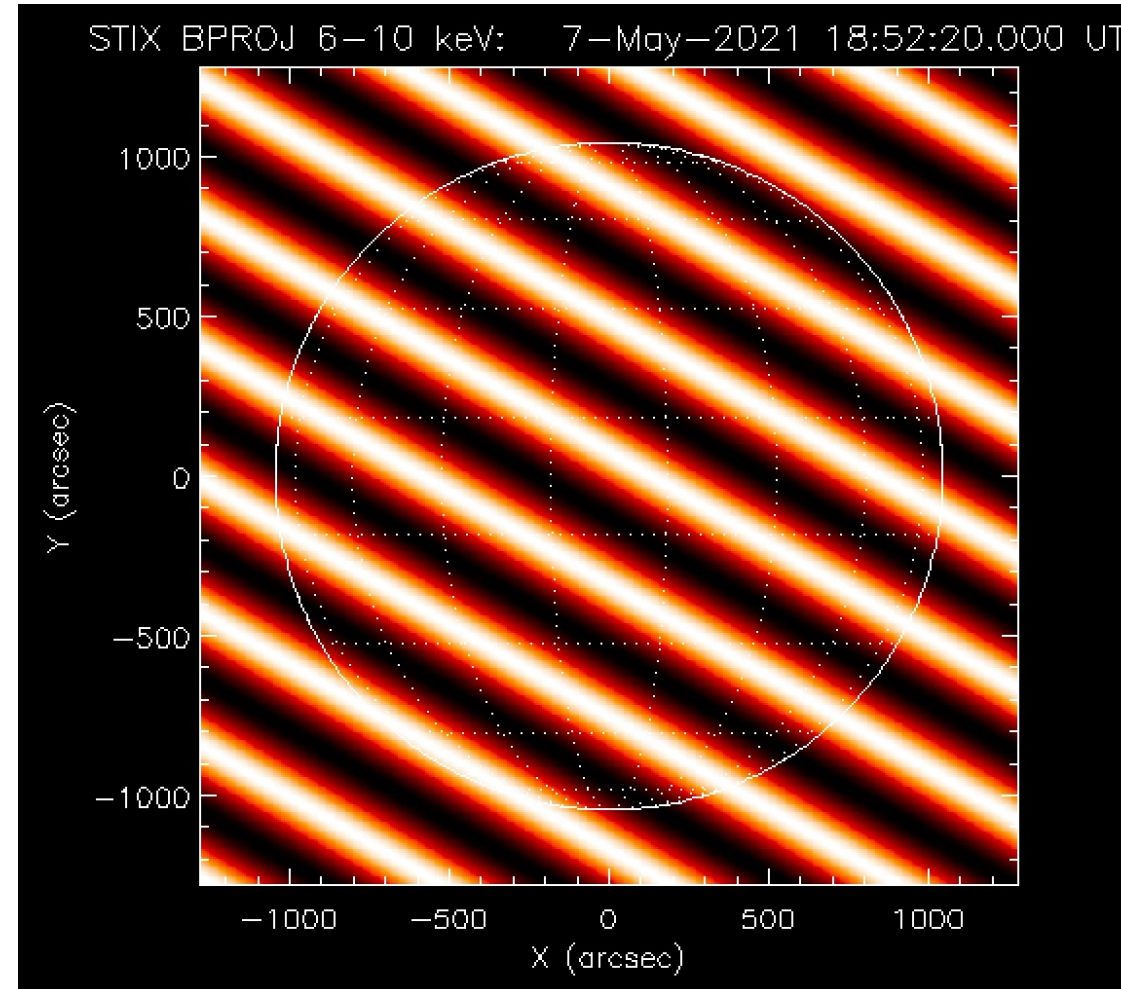


8c



# Back projection (Mertz et al., 1986)

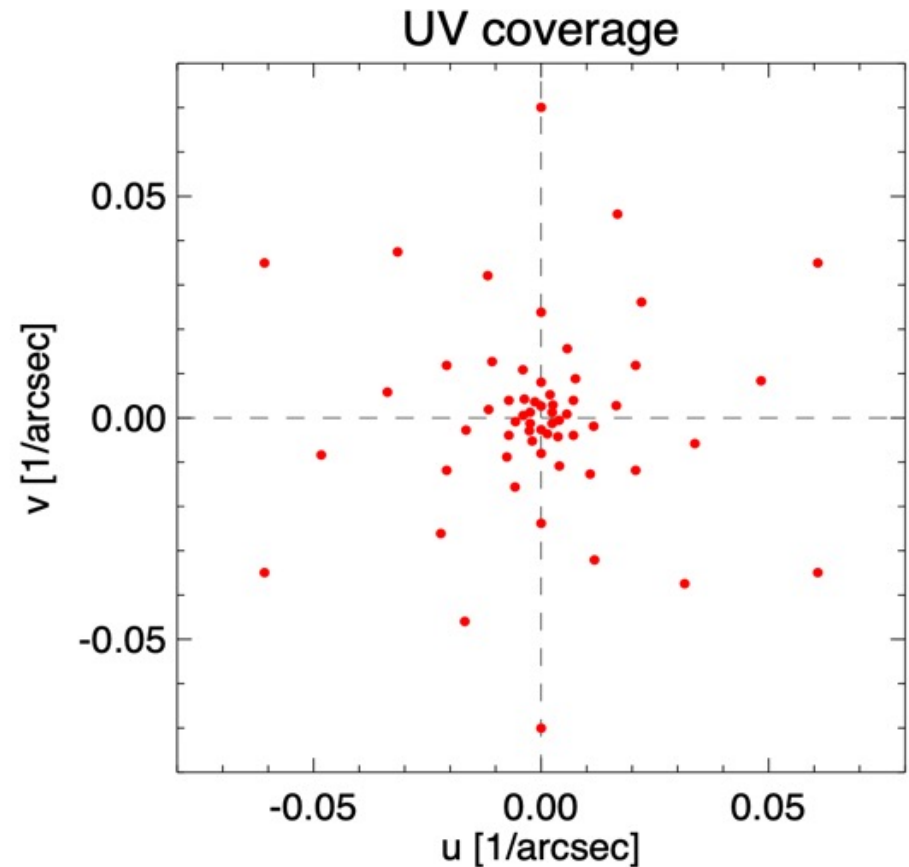
The back projected map is obtained by summing the waves corresponding to all the detectors



# Back projection (Mertz et al., 1986)

Parameters: sinusoidal waves  
weights (keyword **uni**)

- **Natural weighting:** weights equal to 1 (default)
- **Uniform weighing:** weights proportional to the distance of the frequency w.r.t. the origin

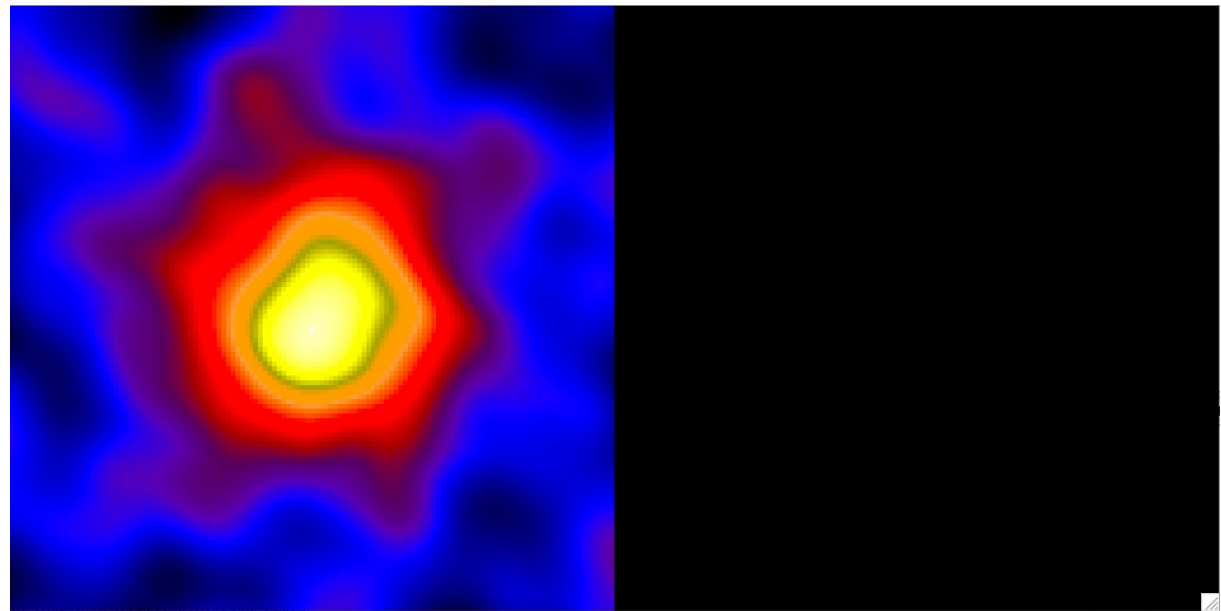


Krucker et al., 2020

# Clean (Högbom, 1974)

Iterative method:

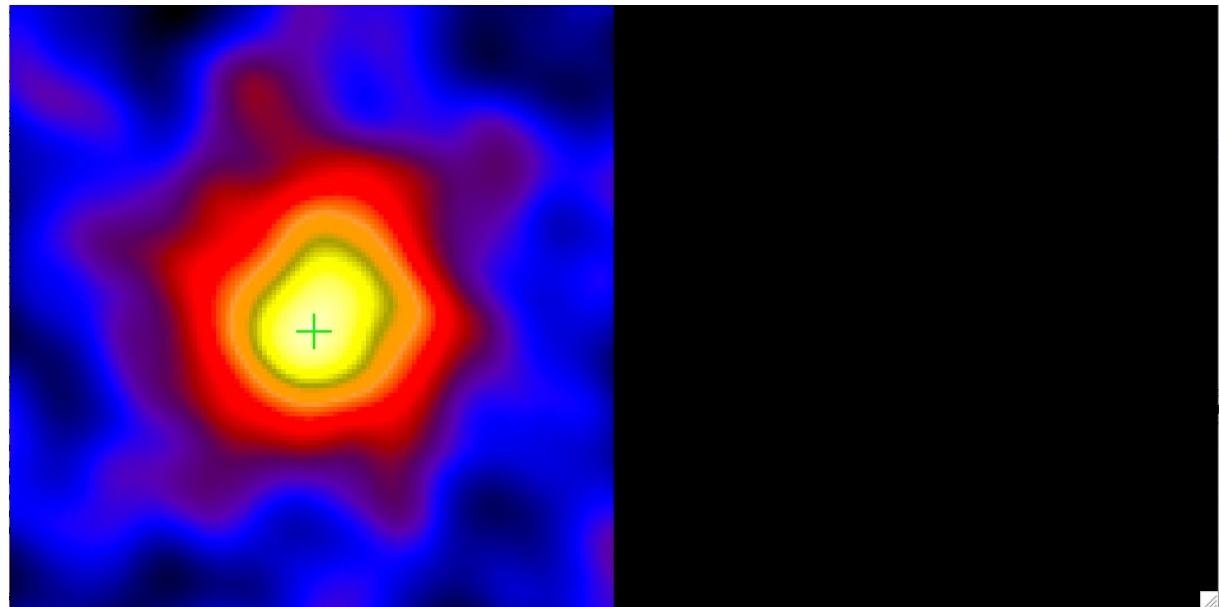
- Creates two maps: **dirty map** (back projection) and **clean components map** (zero map)



# Clean (Högbom, 1974)

Iterative method:

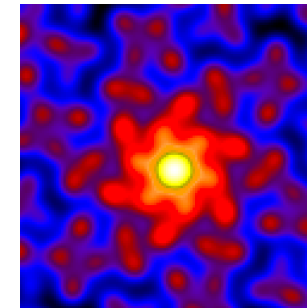
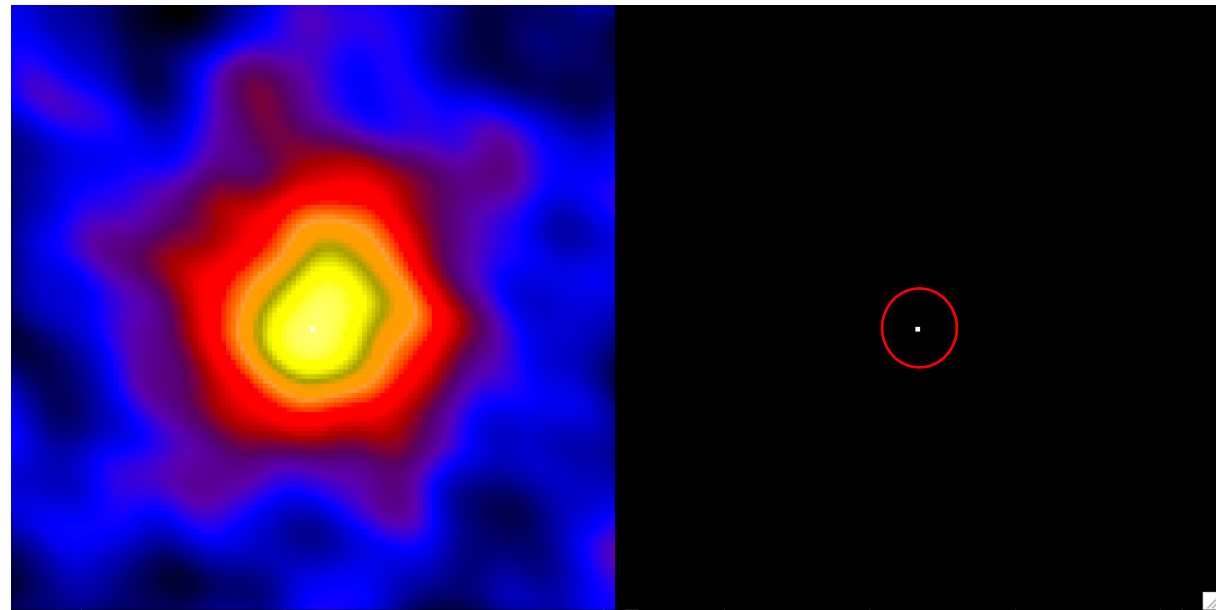
- Creates two maps: **dirty map** (back projection) and **clean components map** (zero map)
- Finds maximum of the dirty map



# Clean (Högbom, 1974)

Iterative method:

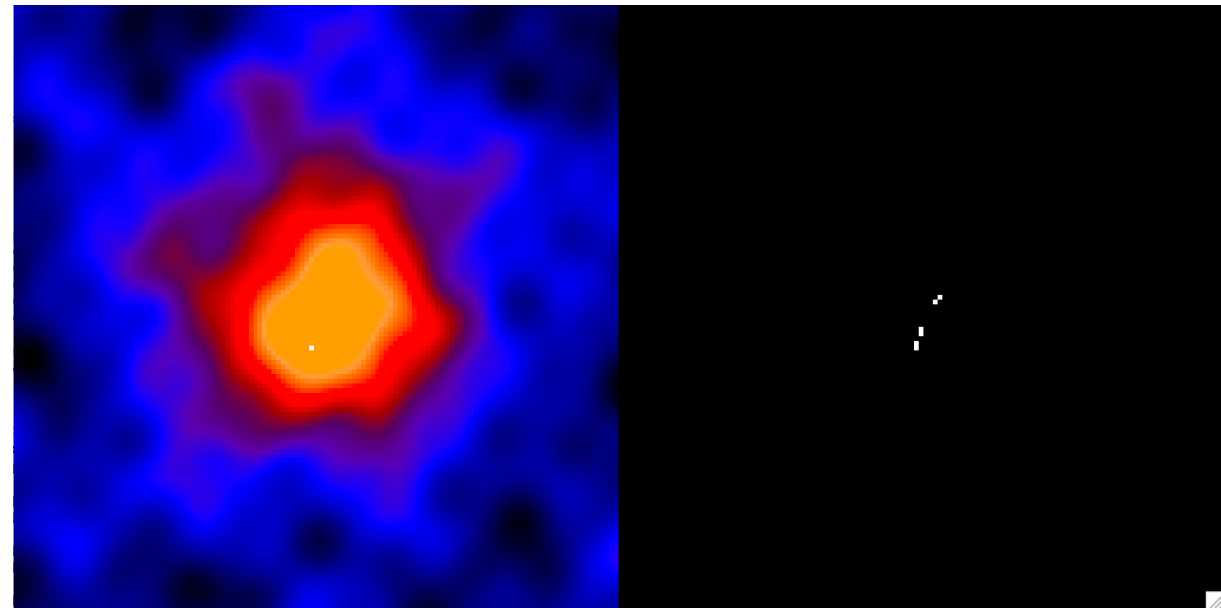
- Creates two maps: **dirty map** (back projection) and **clean components (cc) map** (zero map)
- Finds maximum of the dirty map
- Subtracts a fraction of the PSF from the dirty map and adds a clean component in the cc map



# Clean (Högbom, 1974)

Iterative method:

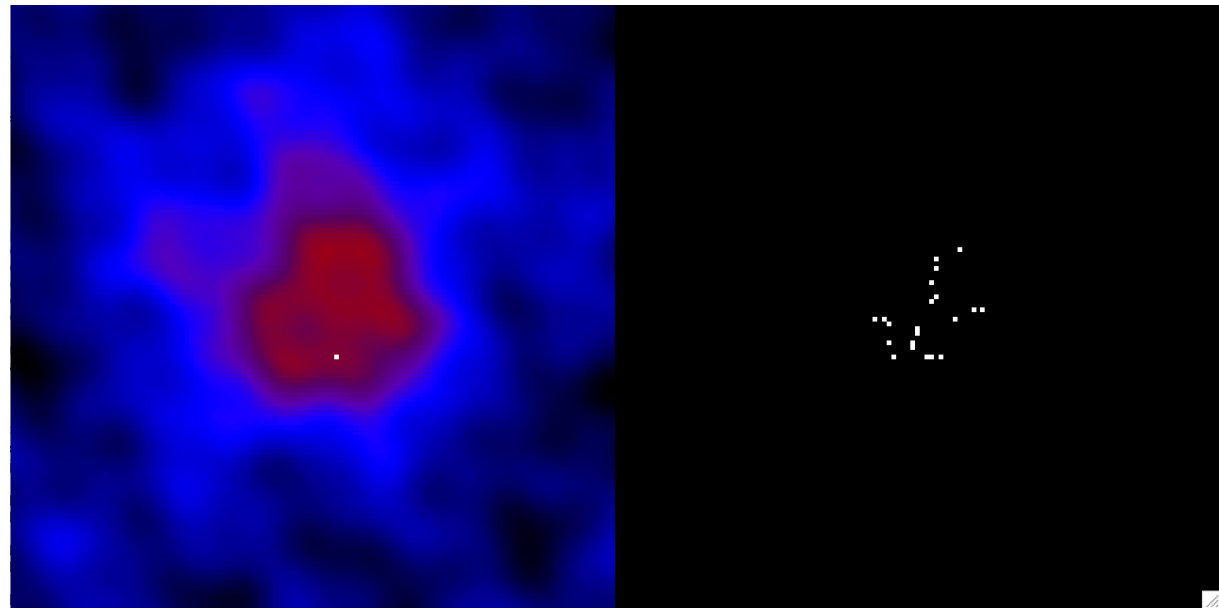
- Creates two maps: **dirty map** (back projection) and **clean components (cc) map** (zero map)
- Finds maximum of the dirty map
- Subtracts a fraction of the PSF from the dirty map and adds a clean component in the cc map
- Iterates



# Clean (Högbom, 1974)

Iterative method:

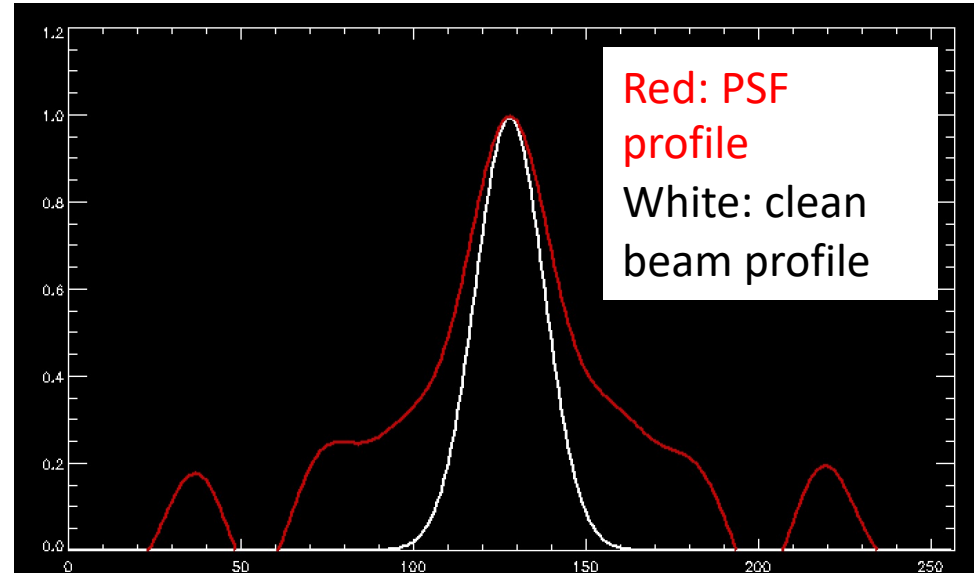
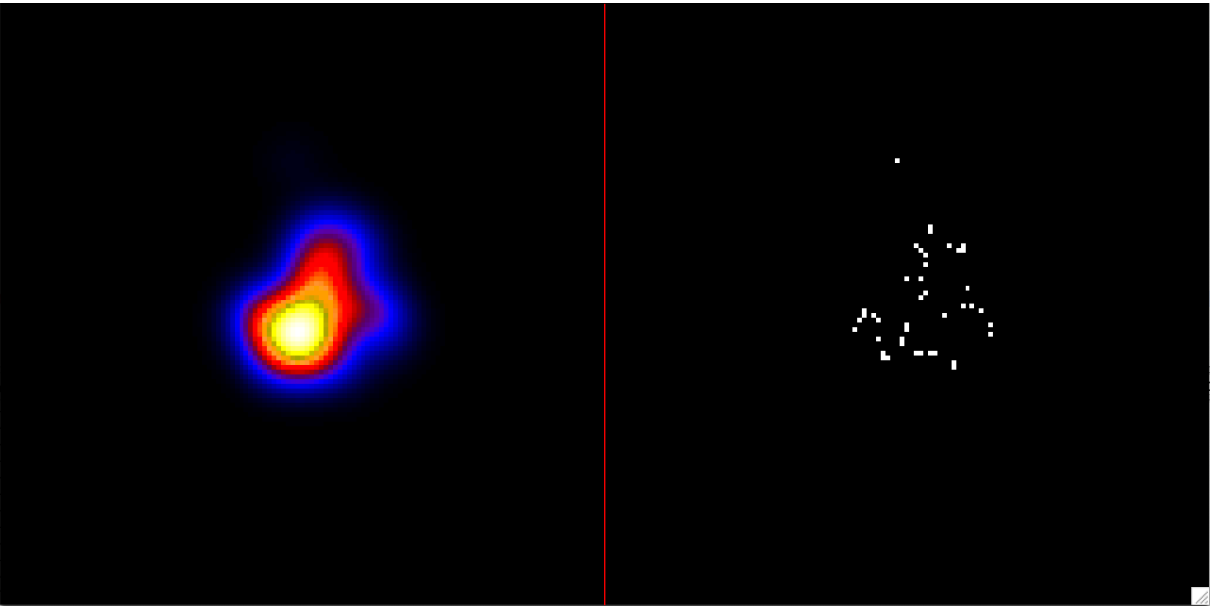
- Creates two maps: **dirty map** (back projection) and **clean components (cc) map** (zero map)
- Finds maximum of the dirty map
- Subtracts a fraction of the PSF from the dirty map and adds a clean component in the cc map
- Iterates



# Clean (Högbom, 1974)

Iterative method:

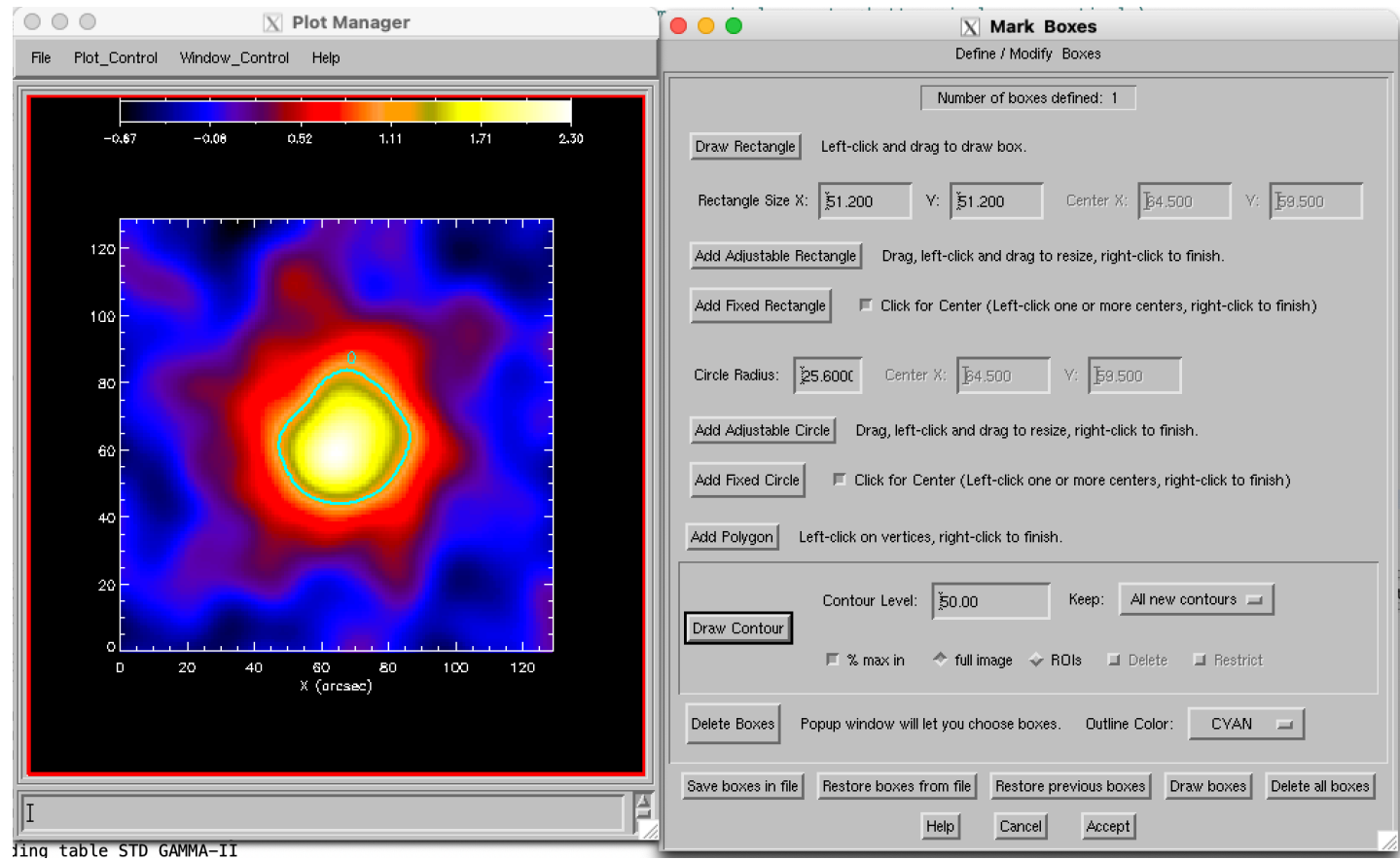
- Creates two maps: **dirty map** (back projection) and **clean components (cc) map** (zero map)
- Finds maximum of the dirty map
- Subtracts a fraction of the PSF from the dirty map and adds a clean component in the cc map
- Iterates
- Final step: convolution and residuals



# Clean (Högbom, 1974)

## Parameters:

- Beam width (so far standard deviation of the Gaussian beam): keyword **beam\_width**
- Clean boxes: keyword **set\_clean\_boxes**
- Back projection weighting: **uniform\_weighting**



# MEMGE (Massa et al., 2020)

Solves the maximum-entropy regularized problem

$$\arg \min_{x \geq 0} \chi^2(x) - \lambda H(x)$$

$$\text{with } \sum_i x_i = f$$

where

$$\chi^2(x) = \sum_i \frac{|(\mathcal{F}x)_i - V_i|^2}{\sigma_i^2} \quad H(x) = - \sum_j x_j \log \left( \frac{x_j}{me} \right)$$

# MEM\_GE (Massa et al., 2020)

Two parameters:

$$\arg \min_{x \geq 0} \chi^2(x) - \lambda H(x)$$

with  $\sum_i x_i = f$

$\lambda$ : regularization parameter (keyword `percent_lambda`)

$f$  : a priori estimate of the total flux (keyword `total_flux`)

# Expectation Maximization (Massa et al., 2019)

- Count-based method

# Expectation Maximization (Massa et al., 2019)

- Count-based method
- EM is the same algorithm as Richardson-Lucy:

$$x_{k+1} = \frac{x_k}{M^T 1} M^T \left( \frac{c}{M x_k} \right)$$

where

$$M(x) = (A_{10a}, B_{10a}, C_{10a}, D_{10a}, \dots)$$

# Expectation Maximization (Massa et al., 2019)

- Count-based method
- EM is the same algorithm as Richardson-Lucy:

$$x_{k+1} = \frac{x_k}{M^T 1} M^T \left( \frac{c}{M x_k} \right)$$

where

$$M(x) = (A_{10a}, B_{10a}, C_{10a}, D_{10a}, \dots)$$

- Advantages: SNR of the counts is higher than the one of the real and imaginary part of the visibilities

# Expectation Maximization (Massa et al., 2019)

- Count-based method
- EM is the same algorithm as Richardson-Lucy:

$$x_{k+1} = \frac{x_k}{M^T 1} M^T \left( \frac{c}{M x_k} \right)$$

where

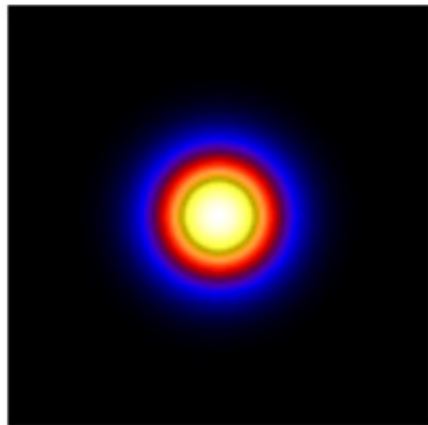
$$M(x) = (A_{10a}, B_{10a}, C_{10a}, D_{10a}, \dots)$$

- Advantages: SNR of the counts is higher than the one of the real and imaginary part of the visibilities
- Parameters: tolerance of the stopping rule (keyword **tolerance**)

# Forward Fit

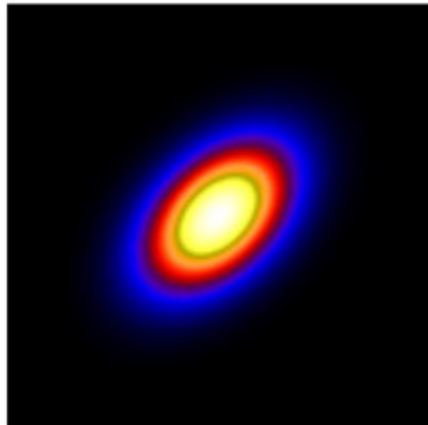
- Parametric source shapes

Circular Gaussian



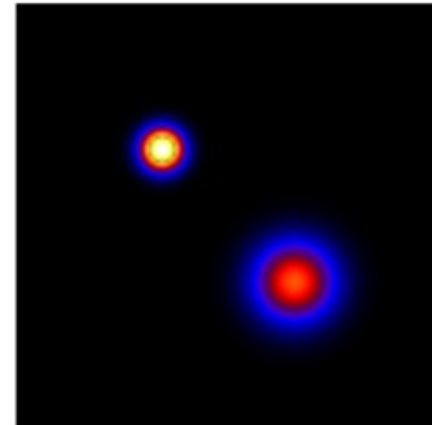
4 parameters

Elliptical Gaussian



6 parameters

Double circular Gaussian

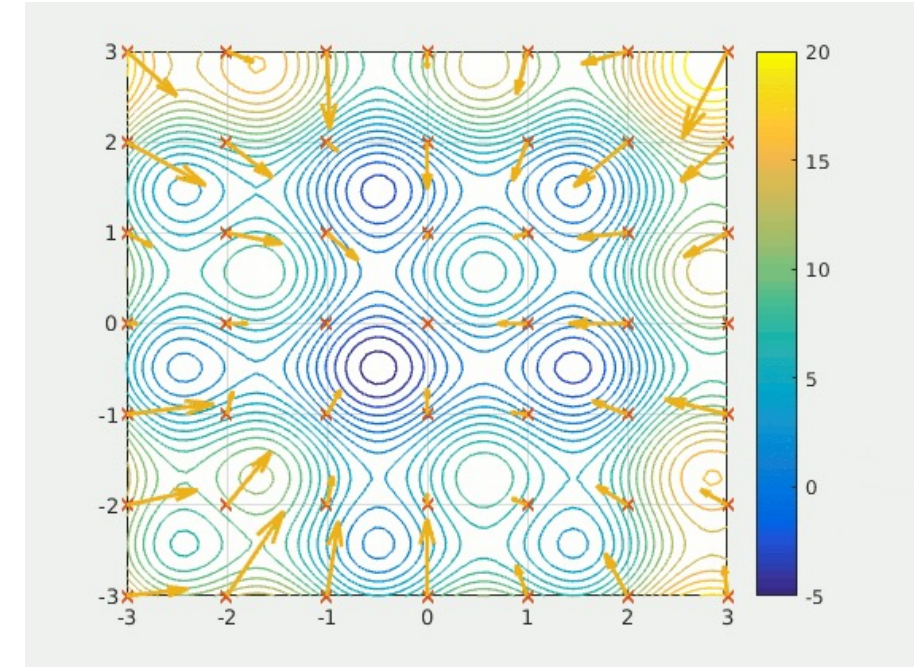


8 parameters

- Solves:  $\arg \min_{\theta} \chi^2(\theta) := \sum_i \frac{|(\mathcal{F}x(\theta))_i - V_i|^2}{\sigma_i^2}$  where  $\theta$  is the array of parameters

# Forward Fit

- **Uncertainty on the parameters:** 20 reconstructions from visibilities perturbed with Gaussian noise and computation of the standard deviation
- Implementation inherited from RHESSI: relies on the AMOEBA\_C routine for the optimization of the parameters (simplex method, sometimes provides suboptimal results)
- **New implementation (available soon):** based on Particle Swarm Optimization (PSO, Eberhart et al., 1995)



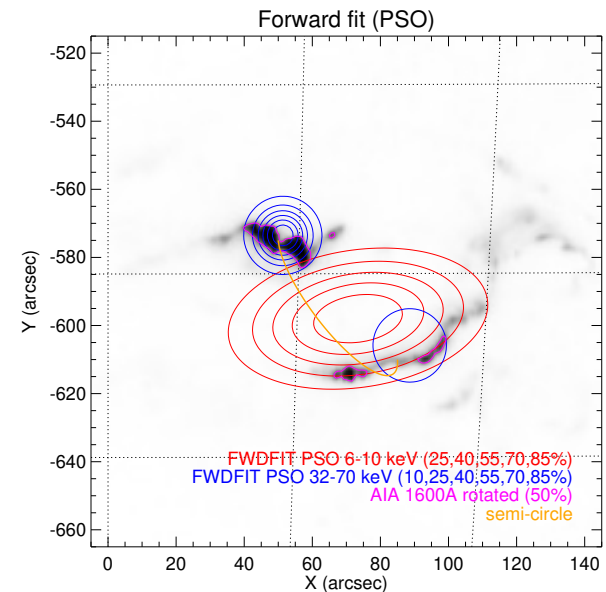
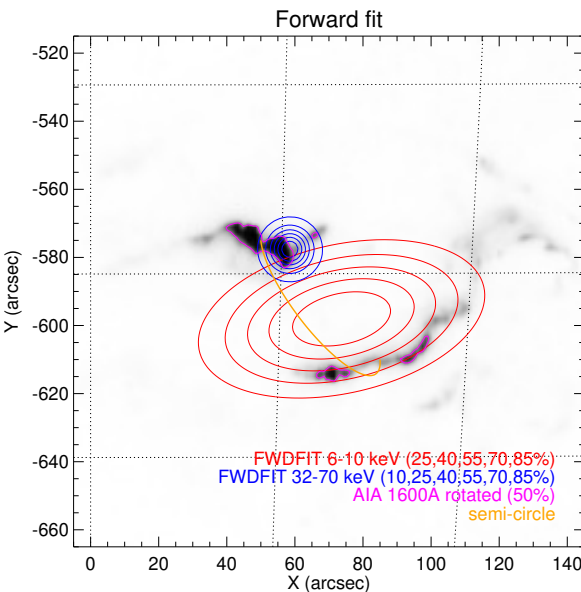
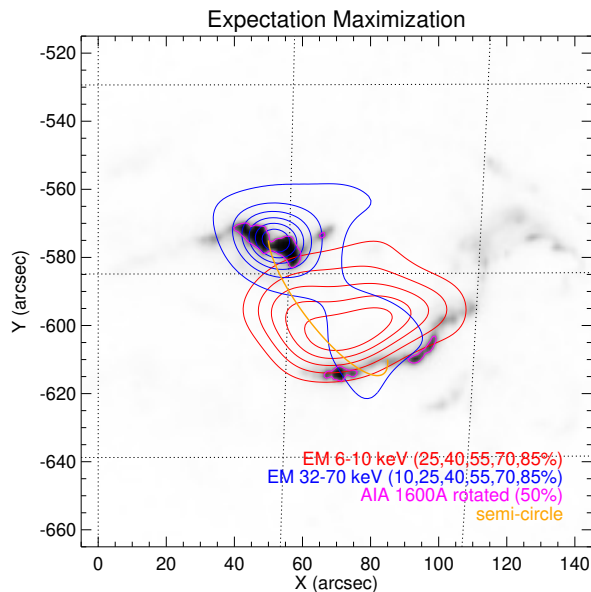
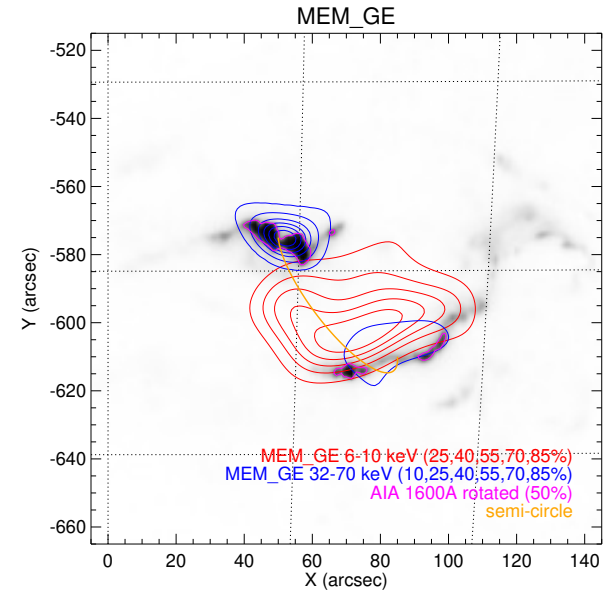
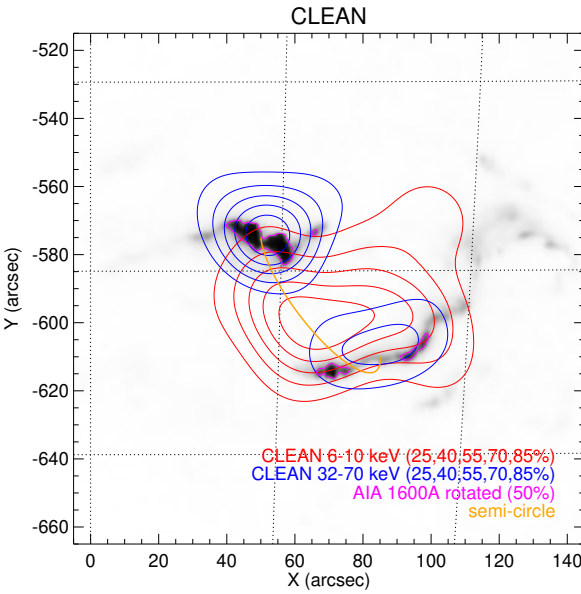
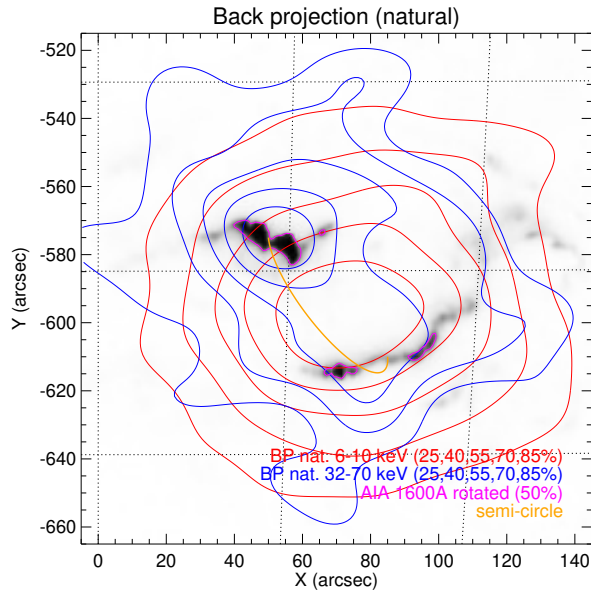
By Ephramac - Own work, CC BY-SA 4.0,  
<https://commons.wikimedia.org/w/index.php?curid=54975083>

# Forward Fit

Parameters to set:

- parametric shape to use for fitting the visibilities (set keyword `shape` equal to `circle`, `ellipse` or `multi`)
- In the new implementation: keyword `uncertainty` for computing the errors on the parameters

# Results - October 28 15:26:00



# Results - October 28 15:26:00

6-10 keV

	X	Y	FWHM max	FWHM min	Angle	Flux
<b>Fwdfit</b>	$80.5 \pm 0.4$	$-594.7 \pm 0.5$	$60.6 \pm 1.5$	$30.8 \pm 0.8$	$33.6 \pm 1.9$	$254.6 \pm 5.9$
<b>PSO</b>	$80.2 \pm 0.5$	$-594.7 \pm 0.3$	$54.3 \pm 0.7$	$28.5 \pm 0.7$	$29.3 \pm 1.4$	$258.2 \pm 4.84$

32-70 keV

		X	Y	FWHM	FLUX
First source	<b>Fwdfit</b>	$59.0 \pm 0.0$	$-581.0 \pm 1.15$	$9.6 \pm 7.7$	$0.33 \pm 0.1$
	<b>PSO</b>	$50.8 \pm 23.5$	$-579.8 \pm 8.9$	$12.6 \pm 8.0$	$0.59 \pm 0.09$
Second source		X	Y	FWHM	FLUX
	<b>Fwdfit</b>	$68.5 \pm 2.98$	$-580.9 \pm 0.7$	$80.0 \pm 6.0$	$0.88 \pm 0.1$
	<b>PSO</b>	$97 \pm 23.8$	$-596.7 \pm 8.8$	$27.0 \pm 6.5$	$0.42 \pm 0.10$

# Next steps

- Improve the absolute location of the reconstructions (using the SAS solution)
- Calibration of the six finest detectors
- Systematic test on large datasets of events for comparing the imaging methods and assessing their performances
- Correction of second order errors in the visibilities
- Implementation of other imaging methods

# Conclusions

- The STIX visibility calibration is completed for collimators 3 to 10
- Several methods are already available for image reconstruction (both count-based and visibility-based)
- The reconstructions are reliable when compared to the AIA maps of the same events and are consistent between different methods

Thanks for the attention!

